RESEARCH ARTICLE SUMMARY

MOSQUITO GENETICS

Ancient origin of an urban underground mosquito

Yuki Haba*, PipPop Consortium, Petra Korlević, Erica McAlister, Mara K. N. Lawniczak, Molly Schumer, Noah H. Rose, Carolyn S. McBride*

Full article and list of author affiliations: https://doi.org/10.1126/science.ady4515

INTRODUCTION: Urbanization is rapidly reshaping landscapes around the world, which poses questions about whether and how quickly animals and plants can adapt. *Culex pipiens* form *molestus*, more commonly known as the London Underground mosquito, has been held up as a benchmark for the potential speed and complexity of urban adaptation. This intraspecific lineage within *Cx. pipiens s. s.* is purported to have evolved human biting and a suite of other human-adaptive behaviors in the subways and cellars of northern Europe within the past 200 years. Form *molestus* features prominently in textbooks as well as scholarly reviews of urban adaptation. Yet, the hypothesis of in situ urban evolution has never been rigorously tested.

RATIONALE: In addition to spawning an enigmatic human-biting form, *Cx. pipiens s. s.* is one of the most important vectors of mosquito-borne disease in temperate regions across the world. The ancestral form of *Cx. pipiens* is bird biting and serves as a major vector of West Nile virus (WNV) within bird populations. Hybridization of this ancestral bird-biting form with human-biting *molestus* produces mosquitoes that are willing to bite both birds and humans and is hypothesized to have driven increasing spillover of WNV to humans in the US and southern Europe over the past two decades. Although this hypothesis has spurred intense efforts to characterize gene flow between forms, the results have been variable and confusing, with no clear consensus on where and to what degree gene flow occurs.

RESULTS: We sequenced the whole genomes of ~350 contemporary and historical *Cx. pipiens* mosquitoes from 77 populations scattered across Europe, North Africa, and western Asia and used population genomic analysis to infer the evolutionary history of *molestus*. Studies of population structure, derived allele sharing, phylogeny, and cross-coalescence show that *molestus* could not have evolved in urban belowground habitats over the past 200 years. Instead, it first adapted to human environments >1000 years ago in the Mediterranean or Middle East, most likely in ancient Egypt or another early agricultural society.

Our genomic data also provide a major revision to our understanding of gene flow between bird- and mammal-biting forms. We found that genetic signatures that researchers previously ascribed to between-form hybridization instead reflect ancestral variation within bird-biting populations. After correcting for this variation, we can see that true hybridization is less common than previously believed and is associated with human population density—a proxy for urbanization.

CONCLUSION: Our work debunks one of the most widely cited examples of rapid urban adaptation—an example that has captured the attention of scientists and laypeople for 25 years. Rather than benchmarking the speed and complexity of urban evolution, this updated history highlights the role of early human society in priming taxa for colonization of modern urban environments. Our work also revises our fundamental understanding of gene flow in this important vector and opens the door to incisive investigation of the potential links between urbanization, hybridization, and arbovirus spillover to humans. □

*Corresponding author. Email: yhaba@princeton.edu (Y.H.); csm7@princeton.edu (C.S.M.)
Cite this article as Y. Haba *et al.*, *Science* 390, eady4515 (2025). DOI: 10.1126/science.ady4515

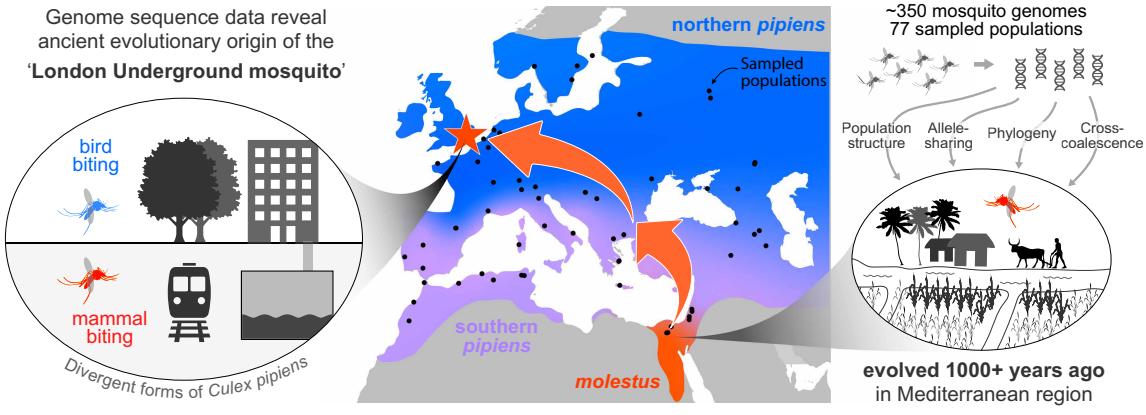

Ancient origin of the London Underground mosquito. A human-biting form of *Cx. pipiens s. s.*, named *molestus*, is found in man-made, belowground habitats across northern Europe, Asia, and North America, but it first became famous in the London Underground subway system. The origins of *molestus* remain elusive, with an oft-cited hypothesis suggesting that it evolved belowground in London <200 years ago. Whole-genome sequencing and population genomic analyses of ~350 mosquitoes densely sampled across the Western Palearctic instead show that *molestus* evolved aboveground in the Mediterranean or Middle East more than 1000 years ago, possibly in association with early agricultural civilizations.

MOSQUITO GENETICS

Ancient origin of an urban underground mosquito

Yuki Haba[1,2]*†, PipPop Consortium‡, Petra Korlević[3], Erica McAlister[4], Mara K. N. Lawniczak[3], Molly Schumer[5], Noah H. Rose[1,2]§, Carolyn S. McBride[1,2]*

Understanding how life is adapting to urban environments represents an important challenge in evolutionary biology. In this work, we investigate a widely cited example of urban adaptation, *Culex pipiens* form *molestus*, also known as the London Underground mosquito. Population genomic analysis of ~350 contemporary and historical samples counters the popular hypothesis that *molestus* originated belowground in London <200 years ago. Instead, we show that *molestus* first adapted to human environments aboveground in the Mediterranean or Middle East over the course of more than 1000 years, possibly in association with ancient agricultural civilizations of the Middle East. Our results highlight the role of early human society in priming taxa for contemporary urban evolution. They also provide insight into whether and how *molestus* contributes to West Nile virus transmission in modern cities.

The rise of modern cities is rapidly reshaping our planet and imposing new selective pressures on the living organisms around us. Many species have begun to adapt to these distinct challenges. A review of the literature highlights at least 130 examples of animals, plants, and microbes that have evolved responses to dense urban environments (*1*). Yet how such adaptations arise and the amount of time that they require to do so remain poorly understood. As urbanization accelerates over the coming decades (*2*), there is a pressing need to better understand the mechanisms and timescale of urban adaptation.

One of the most widely cited examples of urban adaptation involves the northern house mosquito *Culex pipiens* Linnaeus 1758 (Fig. 1A). *Cx. pipiens* is common in temperate zones across the world (*3*, *4*). In Europe and North America, an ancestral form has long been known as a bird-biting mosquito that requires open space for mating (i.e., will only mate readily outdoors) and pauses reproduction (i.e., diapauses) during the cold northern winter (Fig. 1, B and C, blue) (*3*). However, a derived, human-biting form thrives in urban belowground environments, such as subways, cellars, and cesspits, and differs from its aboveground counterpart in ways that seem perfectly suited to subterranean life (Fig. 1, B and C, red) (*3*). The belowground mosquitoes are able to mate in confined, indoor spaces and remain active in winter. Adult females readily bite humans and other mammals. Yet if hosts are scarce, they can develop a first clutch of eggs without taking any blood, a trait known as autogeny. Despite this array of genetically based behavioral and physiological differences, the two mosquitoes show no consistent morphological differences (*3*). They are formally considered distinct forms: the bird-biting *Cx. pipiens* f. *pipiens* Linnaeus 1758 and the human-biting *Cx. pipiens* f. *molestus* Forskål 1775 (*5*), hereafter referred to as simply *pipiens* and *molestus*, respectively.

The sophisticated adaptations of *molestus* to urban belowground environments have led to much speculation over when and where the form originated. A widely cited hypothesis suggests that *molestus* evolved in the London Underground subway system, where it first became famous in the 1940s (*1*, *6*–*11*). During World War II, many Londoners took nightly refuge in the city's subway system to escape intense Nazi bombing. Sleeping on subway platforms protected people from bombs but made them easy targets for *molestus*, which became known as the London Underground mosquito and was hypothesized to have evolved there during the ~100-year period between subway tunnel construction and mosquito discovery (Fig. 1D, left) (*6*, *12*). A London Tube origin is unlikely because *molestus* was reported in cellars and cesspits in France, Denmark, Germany, and the former USSR 10 to 25 years before its discovery in London (*3*, *13*–*15*), but an urban, belowground origin in northern Europe within the past few hundred years remains possible. Recent reviews have pointed to *molestus* as one of the best candidates for rapid urban adaptation (*1*, *7*–*11*), and major science news outlets have treated this hypothesis as fact (*16*–*21*). The idea that a new, reproductively isolated urban taxon with divergence in multiple, complex behaviors could emerge de novo in just a few hundred years is striking and sets a new bar for the number and complexity of changes that we might expect to occur in modern cities over short timescales.

An alternative hypothesis, which is mentioned in the literature but less prominent, posits that *molestus* first adapted to humans in an aboveground context, long before the rise of modern cities (Fig. 1D, right) (*22*, *23*). Although *molestus* is confined to belowground habitats in cold regions, it thrives aboveground in warmer climates, particularly in the Mediterranean basin (*23*). Moreover, early records document *molestus*-like mosquitoes breeding and biting humans aboveground in Egypt, Croatia, and Italy 50 to 100 years before they were discovered in basements and subways (*24*–*26*). According to this alternative scenario, many of the traits that allow *molestus* to thrive in urban belowground environments would represent exaptations, or traits that first arose in a different time and context (*27*). An aboveground Mediterranean origin could also push the timing of *molestus*'s origin back thousands of years, to an era when humans first started forming dense agricultural communities. Early allozyme and microsatellite studies indicate that contemporary *molestus* populations from aboveground and belowground habitats are genetically related (*22*, *28*), but the validity and timing of a putative aboveground origin remain to be tested.

In this work, we leverage the first large population genomic dataset for *Cx. pipiens* to infer when, where, and in what ecological context *molestus* first evolved. Beyond its enigmatic origins, *molestus* is a competent disease vector. Aboveground *molestus* served as the primary vector of a human-specific filarial nematode prevalent in Egypt throughout the 1900s (*3*, *23*). *molestus* is also implicated in the transmission of West Nile virus (WNV) and other arboviruses across Eurasia and North America over the past several decades (*29*, *30*). Solving the mystery of *molestus*'s origins thus has important implications for understanding both rapid urban adaptation and emerging threats to human health.

Form *molestus* is genetically isolated from *pipiens* across the Western Palearctic

Multiple lines of evidence indicate that *molestus* first split from *pipiens* somewhere in the Western Palearctic (a region that includes Europe, North Africa, and western Asia) (*31*) before spreading to other parts of the world. However, the structure of populations across this region has been difficult to decipher owing to the absence of morphological differences. Analysis of one or a small number of genetic loci shows that the two forms are isolated in northern Europe, where harsh winters

[1]Department of Ecology and Evolutionary Biology, Princeton University, Princeton, NJ, USA. [2]Princeton Neuroscience Institute, Princeton University, Princeton, NJ, USA. [3]Wellcome Sanger Institute, Hinxton, UK. [4]Department of Life Sciences, The Natural History Museum, London, UK. [5]Department of Biology and Howard Hughes Medical Institute, Stanford University, Stanford, CA, USA. ***Corresponding author. Email: yhaba@princeton.edu (Y.H.); csm7@princeton.edu (C.S.M.)** †Present address: Zuckerman Mind Brain Behavior Institute and Howard Hughes Medical Institute, Columbia University, New York, NY, USA. ‡All PipPop Consortium authors and affiliations are listed at the end of this paper. §Present address: Department of Ecology, Behavior, and Evolution, School of Biology, University of California San Diego, La Jolla, CA, USA.

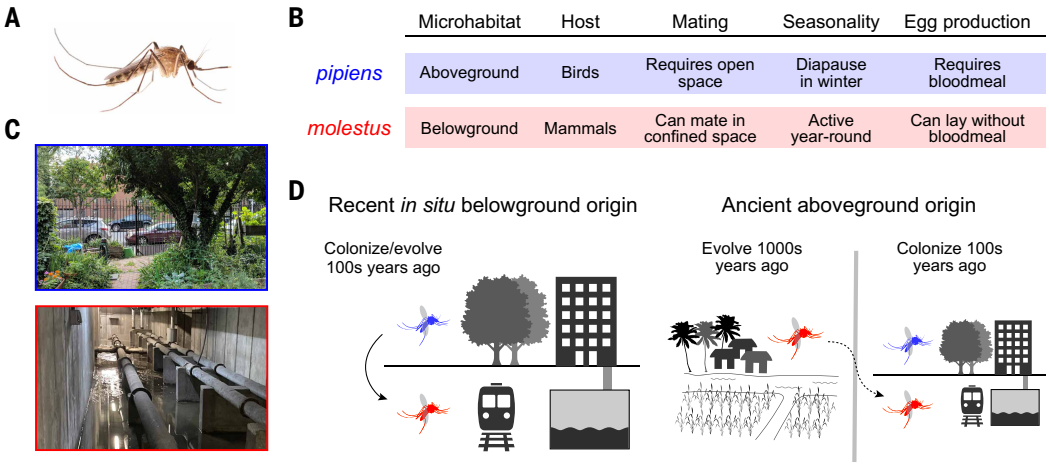

Fig. 1. *Cx. pipiens* form *molestus* behavior, ecology, and hypothetical origin. (**A**) Female *Cx. pipiens* complex mosquito. (**B**) Behavioral and physiological characteristics of *Cx. pipiens* forms in northern Eurasia. At warmer latitudes, *molestus* can breed aboveground. (**C**) Example microhabitats: a city park (*pipiens*) and the flooded basement of an apartment complex (*molestus*). (**D**) Two hypotheses describing *molestus*'s origin. Hypothesis 1 (left) posits that belowground *molestus* evolved from local aboveground *pipiens* in situ within the past 100 to 200 years. Hypothesis 2 (right) posits that *molestus* first evolved in an aboveground context thousands of years ago, possibly in association with early agricultural societies of the Mediterranean basin, with colonization of belowground habitats (dotted arrow) occurring much later (*22*,*23*). [Photos by Lawrence Reeves (mosquito); Yuki Haba (city park); Colin Malcolm (flooded basement), licensed under CC-BY]

confine *molestus* to belowground environments (*22*, *23*). However, *molestus* and *pipiens* appear to be more genetically similar in southern Europe, where both breed aboveground, and the two forms may even collapse into a single panmictic population in North Africa (*22*, *23*). To better resolve the situation with high-resolution genomic data, we sequenced the whole genomes of 357 *Cx. pipiens* individuals collected in 77 locations scattered across the Western Palearctic (Fig. 2A; $n = \sim 5$ individuals per population at 12.9× median coverage). These data are part of a larger collection of 840 genomes to be presented in a companion study of the deeper evolutionary history of *Cx. pipiens* across its entire global range (*32*) (figs. S1 to S3).

We used a principal components analysis (PCA) to assess variation across the Western Palearctic using 504,000 high-quality single-nucleotide polymorphisms (SNPs) (*32*) (Fig. 2B). The first major axis (PC1) accounted for by far the most variation (39.5%; fig. S4A) and cleanly separated belowground and aboveground samples from northern latitudes (Fig. 2C). PC1 thus represents divergence between *pipiens* and *molestus*. Sequenced mosquitoes with known biting or egg-laying behavior ($n = 13$), including those from lower latitudes, were also arrayed across PC1 according to expected form (fig. S5A). PC2 explained ~4% of genetic variation across the sample (Fig. 2B) and was strongly correlated with longitude (fig. S4B).

Our sample included aboveground mosquitoes from London, which clustered with other northern European *pipiens*, but we were not given permission to collect mosquitoes in the London Underground. To confirm that the genetic picture today reflects the one present when iconic World War II populations were first discovered, we used a minimally destructive approach (*33*) to extract and sequence DNA from 22 museum specimens collected at 15 sites in London between 1940 and 1985 (table S2; mean genome-wide coverage = 5.8×). Metadata for most samples did not specify microhabitat, but the sampling locations included the sites of major underground stations, including Paddington, Monument, and Barking. A joint PCA with contemporary samples placed the historical London specimens in the same two genetic clusters that characterize mosquitoes at that latitude today (Fig. 2C, inset, and fig. S5B). We conclude that the genetic character of *pipiens* and *molestus* populations in northern Europe has been stable for the past 75 years.

Form *pipiens* and form *molestus* are genetically well separated in the north, but our data confirm that they are less distinct at southern latitudes. Mosquitoes on both the *molestus* and *pipiens* ends of the PC1 axis have increasingly intermediate values as one moves from northern Europe toward Africa, creating a U-shaped pattern when PC1 is plotted against latitude (Fig. 2C). Notably, however, they never completely merge; even southern populations fall into two discrete genetic clusters with a break at PC1 ~ 0.04 (Fig. 2C, dashed line). Moreover, individuals from these two clusters were frequently collected in the same traps, which highlights the absence of microgeographic barriers (Fig. 2D). Our whole-genome data thus show unequivocally that *pipiens* and *molestus* are able to coexist in sympatry across the region (*34*, *35*). They are genetically closer in the south, and several individuals in our sample may represent early-generation hybrids (e.g., see asterisk in Fig. 2C). Despite this, we see no evidence of collapse into a panmictic population.

Ancestral latitudinal gradient within *pipiens* suggests that *molestus* arose at the southern edge of the Western Palearctic

The genetic similarity of *molestus* and *pipiens* at southern latitudes is believed to result from increased gene flow (*22*, *23*); hybridization should be rare in the north, where the two forms occupy different microhabitats, but increasingly common in the south, where both forms breed aboveground (Fig. 3A). To test this hypothesis, we examined the latitudinal cline within *pipiens*, which is much stronger than that within *molestus* (Fig. 2C). More specifically, we used genome-wide *f3* statistics (*36*) to model each *pipiens* population as a mix of "pure" *pipiens* and *molestus* reference populations taken from their northern extremes. Many European and west Asian populations showed evidence of mixing (Fig. 3B), but the signal was not latitudinal [Fig. 3C; Pearson's correlation coefficient (r) = −0.022, $P = 0.90$]. Moreover, North African *pipiens* populations, which are genetically closest to *molestus*, showed no signs of admixture (Fig. 3B). These results cast doubt on the long-standing hypothesis that latitudinal variation within *pipiens* is driven by hybridization with *molestus*.

An alternative hypothesis, which has not been explored in the literature, is that the latitudinal gradient within *pipiens* predates the evolution of *molestus*. In this case, southern *pipiens* could be genetically closer to *molestus* not because they mix with *molestus*, but because they gave rise to *molestus* (Fig. 3D). Consistent with this idea, we found that southern *pipiens*—and especially *pipiens* populations

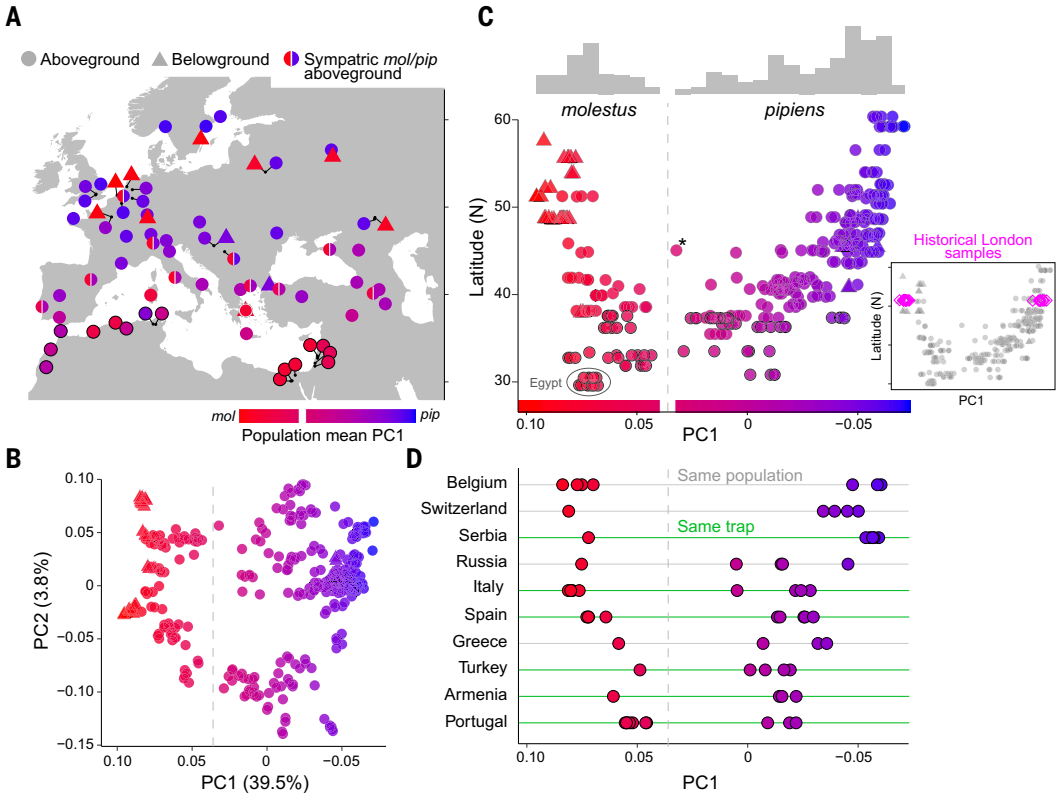

Fig. 2. Form *molestus* is genetically isolated from *pipiens* across the Western Palearctic. (**A**) Sampled populations, colored by average PC1 value. Circles and triangles represent aboveground and belowground locations, respectively. Half-circles indicate that both *pipiens* and *molestus* were collected in the same or nearby aboveground sites. (**B**) PCA of genetic variation across all samples in (A) ($n = 357$). (**C**) PC1 values plotted against latitude, with marginal frequency histogram at top. The gray dashed line indicates a natural break in the histogram, inferred to separate *pipiens* and *molestus* (PC1 = 0.04). Thick outlines mark individuals from North Africa and the Middle East. The asterisk marks a putative F1 hybrid from southwest Russia (Stavropol). (Inset) Position of historical London samples in a combined PCA with contemporary mosquitoes ($n = 22$, collected 1940 to 1985; see also fig. S5). (**D**) PC1 values for *pipiens* and *molestus* individuals collected in the exact same day and trap (green lines) or in the same general location (within 5 to 45 km; gray lines).

in the Mediterranean basin—share as many, or more, derived alleles with a reference *molestus* population from the north as they do with a reference *pipiens* population from the north (Fig. 3E). Moreover, the overall signal of relative allele sharing was strongly latitudinal (Fig. 3F; Pearson's $r = 0.88$, $P = 2.5 \times 10^{-14}$). Taken together, we conclude that the latitudinal gradient within *pipiens* is ancestral—perhaps reflecting adaptation to variation in temperature and/or precipitation—and that *molestus* is most likely derived from populations in the south.

Form *molestus* evolved thousands of years ago in the Mediterranean region

We further explored the geography of *molestus*'s origin by constructing a distance-based (*Dxy*) tree for *Cx. pipiens* individuals from the full global sample (*32*). Contemporary gene flow can obscure ancestral relationships in phylogenetic trees. We were therefore careful to exclude any population or individual that showed signs of recent introgression from the other form (based on *D* and *f*-branch statistics; figs. S6, S7, and S11) or from *Culex quinquefasciatus*, a tropical sibling species that hybridizes with *Cx. pipiens* in the Americas and Asia (based on NGSadmix analysis) (*32*). We also excluded low-coverage samples (<10×). The remaining 204 mosquitoes provided broad coverage across the Western Palearctic and included smaller numbers of representatives from other geographic regions.

The resulting tree provided strong support for an aboveground Mediterranean origin of *molestus*. First, all *molestus* samples formed a monophyletic clade that was nested within Mediterranean *pipiens* (Fig. 4A and fig. S8). Second, the earliest branching lineages within *molestus* corresponded to aboveground mosquitoes from the eastern Mediterranean—specifically Egypt, Israel, and Greece (Fig. 4A). Egyptian and Israeli samples were also among the most genetically diverse, together with two populations from the Caucasus region (Armenia and southern Russia) (Fig. 4B). Finally, whereas belowground *molestus* from northern latitudes formed tight, derived clades, aboveground *molestus* populations from North Africa, the Middle East, and southern Europe were scattered across the base of the tree (Fig. 4A).

Across the Mediterranean region, the Middle East is a particularly compelling location for the emergence of *molestus* because it is the only place within the Western Palearctic where *molestus* is known to occur on its own, in the absence of *pipiens* (Fig. 2A) (*28*, *37*). The Middle East was also home to some of the earliest agricultural societies, which were thriving in Mesopotamia and Egypt by 3000 BCE (*38*). A Middle Eastern origin thus raises the possibility that *molestus* first adapted to human hosts and habitats in isolation from *pipiens* and on a timescale of thousands, rather than hundreds, of years (Fig. 1D, right) (*22*, *23*).

We explored the timing of *molestus*'s origin using a cross-coalescent analysis of DNA haplotypes from Middle Eastern *molestus* (Egypt) and Mediterranean *pipiens* (Morocco) ($n = 2$ individuals with ~50× coverage from each population) (*39*). As expected, the relative cross-coalescence (rCC) rate starts near zero in the recent past, when the two populations are isolated, but rises monotonically and eventually plateaus near one, going backward in time, when they merge into a single

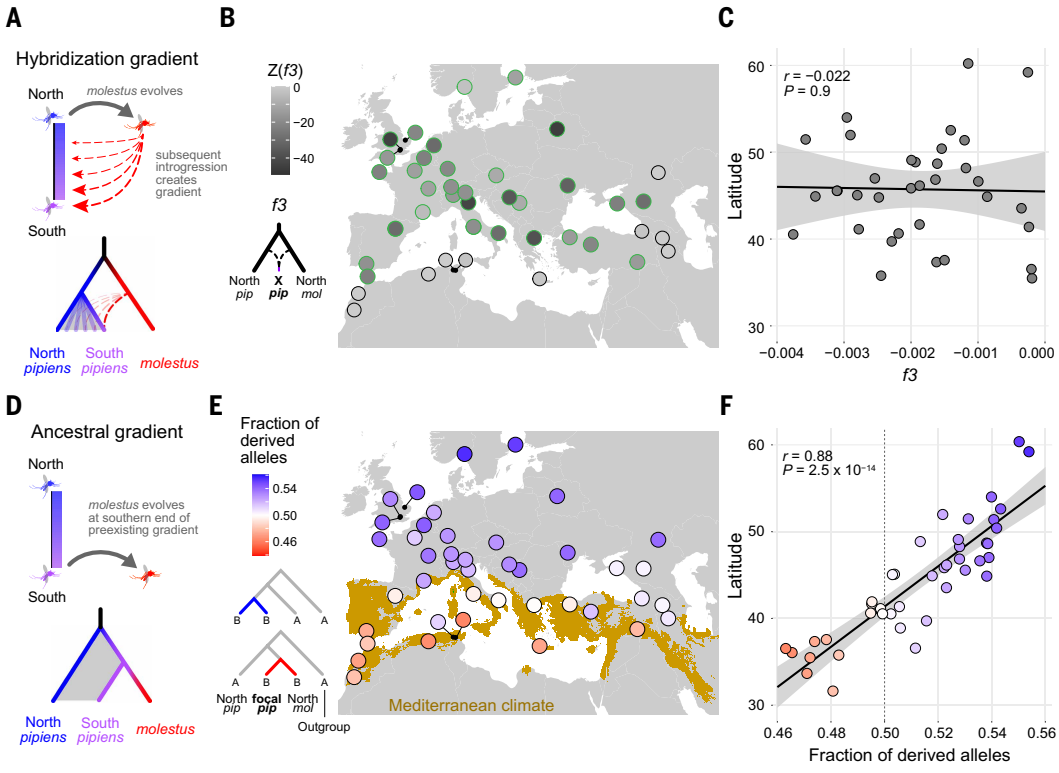

Fig. 3. Ancestral latitudinal gradient within *pipiens* suggests that *molestus* arose at the southern edge of the Western Palearctic. (**A**) Hybridization gradient hypothesis: The genetic gradient within *pipiens* may result from increasing levels of gene flow with *molestus* as one moves from north to south. (**B**) *Z* scores of genome-wide *f3* values for each *pipiens* population when modeled as a mixture of northern *pipiens* (Sweden) and northern *molestus* (Belgium). Significantly negative *f3* values ($Z < -3$; green outlines) are consistent with the presence of admixture. (**C**) *f3* statistics of *pipiens* populations with significant signs of admixture, plotted against latitude. (**D**) Ancestral gradient hypothesis: The genetic gradient within *pipiens* may be ancestral, with *molestus* evolving from southern *pipiens* populations. (**E** and **F**) Fraction of derived alleles shared by each *pipiens* population with northern *pipiens* versus northern *molestus*, shown on a map (E) or as a function of latitude (F). The trees in (E) illustrate two alternatives for a derived allele B, which may be shared by the focal population with one of the two northern forms. The other northern form has the ancestral allele A, present in outgroup *Cx. torrentium*. Red and blue circles mark *pipiens* populations that shared more derived alleles with northern *molestus* versus northern *pipiens*, respectively. Light brown color in (E) highlights the Mediterranean climate zone. Both (C) and (F) include a linear regression line with 95% confidence interval and Pearson's correlation test statistics. Across all analyses, only populations with four or more individuals were included.

ancestral population (Fig. 4C). Accurate assignment of dates to this rCC curve requires knowledge of the de novo mutation rate (μ) and generation time (*g*), neither of which has been directly measured for *Cx. pipiens* in nature. However, plausible literature estimates for μ (4.85×10^{-9}) and *g* (20 days) (*32*) suggest that peak rates of divergence occurred ~2000 years ago (Fig. 4C, dashed arrow), whereas minimum and maximum reasonable values (*32*) lead to split times anywhere between 1300 and 12,500 years ago (Fig. 4C, gray arrowheads). We obtained a similar range of split times when using an alternative *pipiens* population from the southern Caucasus region (Armenia; fig. S10). The temporal resolution of these inferences is limited, and the haplotype phasing that underlies them adds additional uncertainty (*32*). Nevertheless, they are inconsistent with a postindustrial origin for *molestus* in northern Europe (Fig. 1D, left) and instead support an ancient origin, most likely associated with early agricultural civilizations of the Mediterranean or Middle East (Fig. 1D, right).

Introgression from *molestus* into aboveground *pipiens* is associated with human density

Recent urbanization did not drive initial evolution of *molestus*, but it may have driven range expansion and increased contact with *pipiens* across the northern hemisphere—contact that is thought to have contributed to the emergence of WNV in human populations over the past several decades (*29*, *30*). WNV is a mosquito-borne virus that primarily infects birds and is effectively amplified within avian populations by bird-biting *pipiens* (Fig. 5A). Spillover to dead-end human hosts can only occur if local *pipiens* mosquitoes are also willing to bite humans, a broadening of biting behavior that may be driven by gene flow from *molestus* in urban areas (*40*–*42*). This idea has spurred efforts to detect and quantify admixture between *pipiens* and *molestus* in natural populations (*23*); yet, we have shown that much of the genetic signal previously attributed to mixing between forms instead represents ancestral variation (Fig. 3). Form *pipiens* likely receives genetic input from *molestus* in some places, but exactly where and to what extent are not known.

We used *f*-branch statistics to reassess levels of gene flow from *molestus* into *pipiens* while controlling for ancestral variation. *f*-branch statistics allow simultaneous quantification of gene flow among multiple branches in a tree (*43*). To account for the sister relationship between forms in the south (Fig. 3D), we specified a fixed tree in which focal *pipiens* populations were genetically closer to *molestus* than to a reference *pipiens* population from the far north (Fig. 5B). Deviations from this topology (i.e., for focal populations from the north) can then be modeled as "gene flow" into the focal *pipiens* population from the northern reference (Fig. 5B, arrow 1). As expected, the resulting signal was strongly latitudinal (Fig. 5C and fig. S11A). The tree also included two potential sources of *molestus* introgression, which allowed us to distinguish them. We could not detect gene flow into any *pipiens*

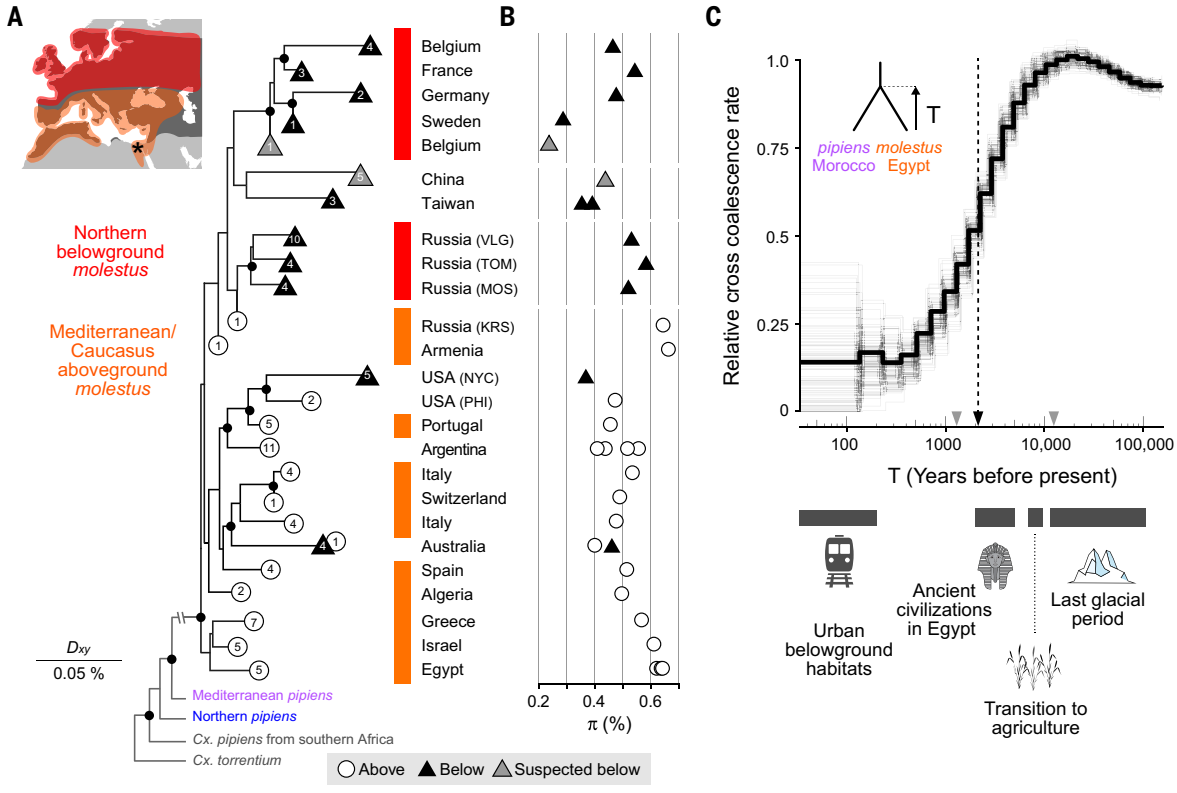

Fig. 4. Form *molestus* evolved thousands of years ago in the Mediterranean region. (**A**) *molestus* clade excerpted from neighbor-joining tree based on pairwise genetic distance (*Dxy*) among putatively unadmixed *pipiens* and *molestus* individuals from the global sample (*32*). Terminal branches are collapsed at the root of each population, with a symbol and number indicating microhabitat and sample size, respectively (*32*). Map inset shows distribution of two subgroups of *molestus* from the tree (orange and red) and *pipiens* (dark gray). Only *molestus* is present in Egypt, marked by an asterisk. Black circles mark nodes with >95% bootstrap support. See fig. S8 for the full tree. (**B**) Genome-wide nucleotide diversity (π) of populations shown in (A). (**C**) rCC rate between Moroccan *pipiens* (MAK) and Egyptian *molestus* (ADR) inferred from phased, whole-genome sequences (*32*). rCC rate is expected to plateau at 1, going backward in time, when populations have merged into a single ancestral population. Rapid divergence is observed between ~10,000 and 1000 years ago, with a split time (T; rCC rate = 50%) of 2141 years (black dashed arrow) based on estimates of generation time and mutation rate (*32*). Biologically reasonable upper and lower bounds for these parameters give minimum and maximum split times of 1298 and 12,468 years (gray arrowheads). Thick black line shows genome-wide result, and light gray lines show 100 bootstrap replicates.

population from the early branching *molestus* lineage in Egypt (Fig. 5B, arrow 2, and fig. S11C), consistent with its isolated location at the southern edge of the contemporary range. However, we detected substantial gene flow into some *pipiens* populations from a derived *molestus* lineage present in the north (Fig. 5B, arrow 3; Fig. 5D; and fig. S11B).

Levels of gene flow from northern *molestus* into *pipiens* did not covary with latitude (Fig. 5D and fig. S11B) but showed a positive association with human population density (*44*–*46*). The more humans living within 1 to 10 km of each sampling location, the more likely we were to observe introgression (Fig. 5E). This relationship was most significant when averaging human density across an area with a 3-km radius [linear regression, $P = 0.003$, coefficient of determination (R^2) = 0.21; Fig. 5, E and F], which suggests that levels of urbanization immediately around collection sites are most predictive of hybridization. Moreover, this signal was driven primarily by the consistent presence of ~5% introgression in truly urban areas, defined by the European Commission as having >1500 people per square kilometer (Fig. 5F) (*47*). Introgression was less predictable at rural sites ($P = 0.07$, $R^2 = 0.11$, excluding urban centers). Inclusion of three statistical outliers in this analysis (Fig. 5F, gray dots) slightly weakened the trend but still indicated a strong association (regression, $P = 0.005$, $R^2 = 0.18$). Notably, a site in Paris showed ~15% introgression, as one might expect on the basis of its density, but we could not detect any genetic input from *molestus* in London. Such geographic variability in levels of gene flow may in part reflect whether local *pipiens* and *molestus* populations are infected by compatible or incompatible strains of *Wolbachia pipientis* bacteria (*48*, *49*). Taken together, our results counter the long-standing idea that gene flow between *pipiens* and *molestus* is greatest at southern latitudes (where both forms breed aboveground) and instead reveal a complex landscape of introgression that is modestly associated with levels of human activity.

Discussion

Understanding how life can adapt to rapid urbanization is an important challenge in evolutionary biology. As examples accumulate in the literature, each case provides a reference for the potential speed and character of adaptation. In this work, we revisit one of the most iconic examples using high-resolution population genomic data. Instead of evolving in the subway system of a northern European city over the course of 100 to 200 years, our results indicate that *Cx. pipiens* f. *molestus* first adapted to human habitats aboveground at Mediterranean latitudes over the course of 1000 or more years (Fig. 6). We cannot say exactly where within this region adaptation first occurred, but biogeographic and archeological evidence point to Egypt as a likely origin. Form *molestus* is particularly abundant in Egypt's Nile basin and occurs there on its own, without *pipiens*. Early agricultural settlements along the Nile would have provided a new "human" niche in

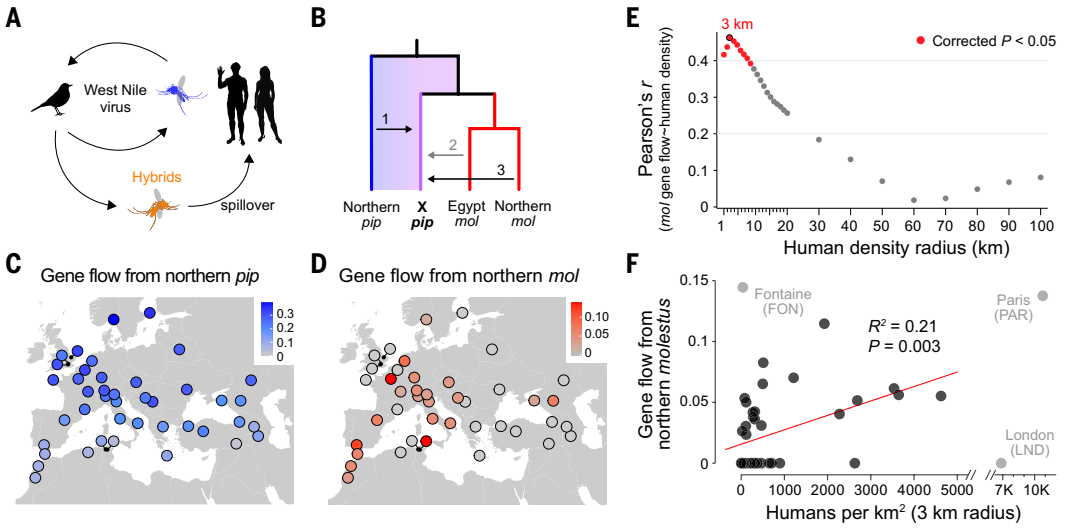

Fig. 5. Introgression from *molestus* into *pipiens* is associated with human density. (**A**) Schematic of WNV transmission dynamics. Form *pipiens-molestus* hybrids, which have intermediate biting preference (*42*), are implicated in the spillover of WNV from birds to humans (*40*, *41*). (**B**) Base tree used to simultaneously estimate three potential sources of introgression into focal *pipiens* populations (X *pip*): northern *pipiens* (Sweden, SWE), Middle Eastern *molestus* (Egypt, ADR), and northern *molestus* (Belgium, BVR). (**C** and **D**) Population-specific estimates of gene flow from northern *pipiens* (C), which accounts for the ancestral latitudinal gradient, and northern *molestus* (D). We did not detect gene flow into any population from Middle Eastern *molestus* (fig. S11C). (**E**) Correlation between gene flow from northern *molestus* (D) and human population density within circles of varying radius around each collection site. (**F**) Gene flow from northern *molestus* as a function of human density within a 3-km radius of each collection site. Three outliers in gray (Cook's distance > 4) were excluded, but regression remains significant if included ($P = 0.005$, $R^2 = 0.18$).

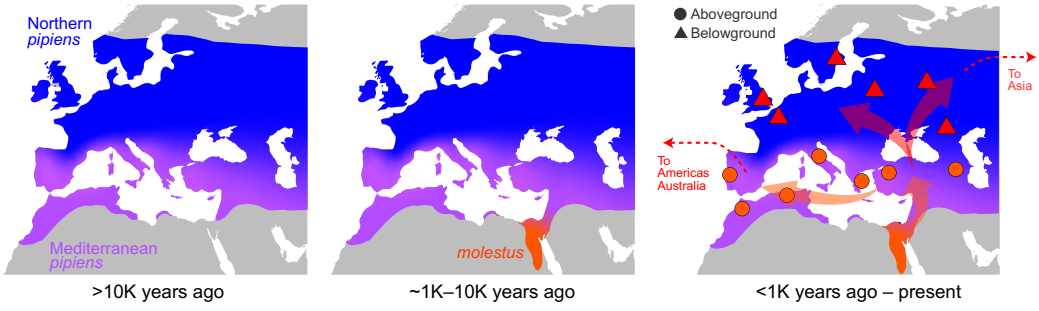

Fig. 6. Inferred evolutionary history of *molestus*. Three sequential panels show the inferred history of *molestus*. (**Left**) The latitudinal genetic gradient characterizing extant *pipiens* populations in the Western Palearctic predates *molestus*. (**Middle**) The rise of dense, settled, and agricultural communities at southern latitudes 2000 to 10,000 years ago, including along the Nile River in Egypt, would have provided new ecological opportunities for mosquitoes that could adapt to human hosts and habitats—driving the evolution of *molestus*. (**Right**) Eventually, *molestus* must have spread north, where it became established alongside *pipiens* in the warm Mediterranean region by the 1800s (but possibly earlier) and in belowground microhabitats of cold, northern cities by the early 1900s. Our distance tree (Fig. 4A) suggests that *molestus* was further spread (most likely by humans) overland all the way to East Asia and from the Mediterranean region overseas to America and Australia.

an area otherwise too arid to support robust *Cx. pipiens* populations. Irrigation systems and latrines offer rich breeding sites for larval stages, and abundant humans and domestic mammals offer a reliable source of blood for adult females. Ancient pharaonic artifacts and papyrus are also consistent with the idea that *molestus* was spreading filarial worms among humans in the Nile basin as many as 2000 years ago (*23*).

Rather than benchmarking the speed and complexity of urban evolution, this updated history highlights the role of preexisting traits, or exaptations, in adaptation to urban environments (*27*). Three of the key behaviors that allow *molestus* to thrive belowground are present in contemporary, aboveground populations in Egypt and almost certainly arose in ancient times: mammal biting, the ability to mate in confined spaces, and the ability to lay a first clutch of eggs without a blood meal (*37*, *50*). A fourth trait, lack of diapause, which limits *molestus* to belowground environments at northern latitudes, is also present in the Middle East today (*37*). Form *molestus* was thus primed to take advantage of northern, belowground environments before they arose. It joins a host of other urban taxa that first became dependent on humans thousands of years ago, including brown rats (*51*), house mice (*52*), cockroaches (*53*), house sparrows (*54*), and the dengue mosquito *Aedes aegypti* (*55*).

Ancient origins do not preclude additional, contemporary evolution (*51*, *53*). Once established belowground, *molestus* was likely exposed to a new suite of challenges. For example, many belowground habitats lack vertebrate hosts altogether, providing a competitive edge to females that can develop eggs without a blood meal. This trait, called autogeny, is present in contemporary Middle Eastern *molestus* but only at low frequency (*37*, *50*). By contrast, it occurs at high frequency in some aboveground *molestus* from southern Europe (*34*) and is nearly fixed in northern belowground populations (Fig. 1B). Future work should explore whether increased autogeny may provide a bona

fide example of rapid, urban evolution in belowground environments and whether this change arose just once or many times in parallel (*56*). Our distance tree (Fig. 4A) suggests that belowground populations from northern Eurasia are all closely related but that those from the east coast of North America (and possibly Australia) represent independent colonization events.

Our findings also carry public health implications. The emergence and spread of WNV over the past two decades have triggered intense interest in quantifying admixture between *molestus* and *pipiens* because hybridization is thought to drive spillover from birds to humans (*40*, *41*). Yet, we show that true patterns of admixture are obscured by ancestral relationships at southern latitudes. For example, it is currently standard practice to identify hybrids using a single locus marker called CQ11 (*57*). Pure *pipiens* and *molestus* were thought to be fixed for different alleles at this locus, such that heterozygotes must be hybrids. We instead suggest that *pipiens* harbors ancestral variation at this locus. The "*molestus*" allele was likely present at moderate frequency in the Mediterranean basin before *molestus* arose and remains present in pure Mediterranean *pipiens* today. Accurate inferences of gene flow will require more substantial genomic data and more complex analytical methods (e.g., Fig. 5).

After accounting for ancestral variation, we show that hybridization between *pipiens* and *molestus* is associated with human activity (Fig. 5E) but is no more common at southern latitudes within the Western Palearctic than it is in the north (Fig. 5D). The latter result suggests the presence of strong reproductive barriers, possibly related to divergence in mating behavior (*35*), that go beyond physical isolation of forms in different microhabitats. Future work should also consider the possibility that Mediterranean *pipiens* populations are somewhat intermediate between canonical northern forms at the behavioral—as well as the genetic—level (*58*). They may be effective bridge vectors even in the absence of genetic input from *molestus*. WNV represents an increasing threat to public health across the northern hemisphere, with many of the most severe outbreaks occurring within the past 5 years (*59*, *60*). Taken together, we hope that our work opens the door to more incisive investigation of the potential links between urbanization, gene flow, ancestral variation, and viral spillover.

Materials and methods

Culex pipiens Population Genomics Project

This study is one of two flagship studies associated with the *Culex pipiens* Population Genomic Project, also known as PipPop. The current study investigates the origins of form *molestus*, whereas the companion study will examine the deeper evolutionary history of the species and global population structure and genomic diversity. Both studies make use of 840 individual whole-genome sequences of *Cx. pipiens* complex mosquitoes (*Cx. pipiens sensu lato*) and outgroups (fig. S1 and table S1). Within the complex, we specifically targeted *Cx. pipiens s. s.* Linnaeus 1758 and hybrids (n = 688), but we also sequenced smaller numbers of *Cx. quinquefasciatus* Say 1823 (n = 101), *Culex pallens* Coquillett 1898 (n = 33), and *Culex australicus* Dobrotworsky and Drummond 1953 (n = 5). *Culex torrentium* Martini 1925 (n = 9) was included as an outgroup, and a handful of sequenced mosquitoes were inferred to belong to more distant, unknown taxa (n = 4; table S1). A total of 790 genomes were sequenced for PipPop, whereas 50 were previously published [40 from (*61*) and 10 from (*62*)].

Mosquito collection: We collected and sequenced 790 mosquitoes from 163 populations spread across 44 countries in the Americas, Europe, Africa, Asia, and Australia, targeting $n \sim 5$ individuals per population (fig. S1 and table S1). 752 mosquitoes (95%) were collected from 2014 to 2021, and the remaining 38 (5%) were collected from 2003 to 2012. Mosquitoes were collected from both aboveground (87%) and belowground (13%) sites. Belowground sites included basements of residential buildings, manholes, stormwater drains, cesspits, subway systems, and underground floors of a parking garage. Aboveground sites spanned a variety of habitats, from dense urban environments to residential areas to natural parks. 786 mosquitoes (99.5%) were wild-caught and 4 individuals (0.5%) came from laboratory colonies originally derived from belowground sites in Amsterdam, Netherlands or Athens, Greece. Of the 786 wild-caught mosquitoes, 462 mosquitoes were collected as adults, 318 as larvae or pupae, and 6 as eggs. Larvae and pupae were collected from dense breeding sites to avoid sampling siblings. Egg samples were reared to adults in the laboratory before sequencing, and only one individual per egg raft was used. Mosquitoes were killed either by submersion in >95% ethanol or snap freezing. Detailed sample metadata, including individual and population IDs, GPS coordinates, collection date, life stage, sex, and trapping method, can be found in table S1.

Mosquito identification: Mosquitoes collected as adults or reared to adults before preservation were identified as *Cx. pipiens sensu lato* (i.e., *Cx. pipiens* species complex) or *Cx. torrentium* (outgroup) using standard morphological metrics. We further confirmed that samples belonged to the *Cx. pipiens* complex or *Cx. torrentium* after DNA extraction (see below) using a multiplex polymerase chain reaction (PCR) targeting the *ace-2* locus (*63*) followed by visual inspection of amplicon sizes on a gel. Samples with no bands or unexpected band sizes were excluded before continuing to library preparation.

DNA extraction and genome sequencing: Genomic DNA was extracted from whole bodies using the NucleoSpin 96 DNA RapidLyse kit (Macherey-Nagel, Germany). After PCR-based species identification (see above), we prepared DNA sequencing libraries using Illumina DNA Prep Kits (Illumina, USA) with custom dual-unique barcodes. Approximately 80 barcoded libraries were pooled and sequenced on individual S4 lanes of a Novaseq 6000 PE150 sequencer (Illumina, USA), with a target genome-wide coverage of 10 to 15× (fig. S1B). However, one pool including Mediterranean and Middle Eastern mosquitoes was sequenced across four S4 lanes (a full flow cell) to achieve higher coverage (~60×) for use in cross-coalescence analyses (fig. S1B).

Sequence data processing and variant calling

See fig. S2 for a schematic summary of our data curation pipeline.

Read processing and mapping: Raw reads were assessed for quality using FastQC v.0.11.8 (*64*), and low-quality bases and adapters were trimmed using Trimmomatic (*65*). Trimmed reads were mapped onto the chromosome-scale CpipJ5 genome assembly for *Cx. quinquefasciatus* (*62*) because a chromosome-scale assembly for *Cx. pipiens s. s.* was not available at the time of analysis. We used BWA-MEM v.0.7.17 (*66*) to map the reads with default settings and identified and removed optical and PCR duplicates with Picard MarkDuplicates v.2.20.2 (*67*). We then used GATK v.3.8 (*68*) to perform local realignment around small insertions and deletions. We calculated genome-wide coverage after deduplication using Mosdepth v.0.3.3 (*69*). We used the deduplicated, realigned reads for all the analyses below.

Identification of accessible regions: We used 50 *Cx. pipiens s. s.* individuals (each with >20× coverage) and 50 *Cx. quinquefasciatus* individuals (each with >10× coverage) to identify regions of the genome with reliable read mapping across the *Cx. pipiens* species complex. More specifically, for each taxon separately, we pooled reads across the 50 individuals and looked for genomic sites with 0.5 to 1.5× normalized coverage, where normalization was based on the species-specific average at coding sites. More than 88% of coding sites fell within this "reliable" coverage window in both species, whereas only ~27% of noncoding sites did so (fig. S3, A and B). Across both coding and noncoding sites, more reads mapped reliably for *Cx. quinquefasciatus* than for *Cx. pipiens s. s.*, as expected given our use of a *Cx. quinquefasciatus*

reference assembly (*62*). The difference was minor for coding sites but more substantial for noncoding sites, of which 60% and 34% showed reliable mapping in *Cx. quinquefasciatus* and *Cx. pipiens s. s.*, respectively (fig. S3, A and B). Notably, although sites with reliable coverage in both species were scattered across the genome, those with reliable coverage in only one of the other species were not randomly distributed (fig. S3C). In particular, several small, discrete regions of chromosomes 2 and 3 showed unexpectedly better mapping in *Cx. pipiens s. s.* than in *Cx. quinquefasciatus* (fig. S3C, right). We suspect that these regions represent small chunks of introgression from *Cx. pipiens s. s.* into the JHB laboratory strain that was used to generate the CpipJ5 assembly. We limited all analyses in this study to sites that showed 0.5 to 1.5× normalized coverage in both species (fig. S3C, left). We further limited our analysis to nonrepetitive sites, as indicated in a RepeatMasker (v 4.0.9) analysis conducted by the authors of the reference assembly (*62*). Taken together, our analyses consider ~131 million accessible sites or ~23% of the total 559–mega–base pair (Mbp) genome.

Variant calling and SNP filtering: We called single-nucleotide variants in all 840 individuals using BCFtools v1.13 (*70*). Variant calling was parallelized across multiple 20-Mb chunks of the genome. In addition to masking the inaccessible sites and repeat elements described above, we also masked multiallelic SNPs, indels, and SNPs falling within 5 bp of indels. This gave us an initial set of biallelic SNPs that fell in the accessible regions. We then calculated key statistics for each SNP and removed those with QUAL < 50, MQ < 50, >10% individuals with missing genotypes, average mean depth across all samples of <10× or >30×, or alleles of GQ < 20. These cutoffs were chosen after inspection of the distribution of each statistic, following GATK hard-filtering best practices for nonmodel species (*71*). After filtering, we were left with 30.6 million high-quality, accessible, biallelic SNPs (of ~131 million total accessible sites). This full SNP set was used for all analyses except where otherwise specified.

Individual filtering: We removed two samples from Raleigh, NC, USA, with <2× coverage and >50% genotype missingness (RAL5, RAL6). We also filtered the full sample set for kin based on pairwise KING kinship coefficients computed in NgsRelate v.2.0 (*72*). Almost all pairs showed low relatedness, as expected (mean kinship coefficient 0.00026; fig. S3D). However, a subset of pairs showed higher values, largely falling in one or more of the following categories: (i) pairs of larvae from the same pool, (ii) pairs from the same belowground collection, and/or (iii) pairs from the same laboratory strain (fig. S3D). We identified all pairs of individuals with kinship >0.09 and excluded the individual with lower coverage. We additionally excluded three individuals (PAR4, OSJi4, and KAV5) that showed unexpectedly high relatedness to many individuals from other populations, and we excluded one individual from Malaysia (MEL5) that clustered with North American samples. The unexpected relatedness of PAR4, OSJi4, and KAV5 to many other individuals could not be explained by their position in the 96-well plates used to process samples nor by low sequence coverage. Although the Malaysian sample could conceivably be a migrant, we chose to remove it out of an abundance of caution.

Final sample set: After filtering low-quality individuals and kin, we were left with 743 unrelated mosquitoes. A few analyses presented here address the full global sample. However, unless otherwise specified, this study focuses on the subset of 357 individuals collected in the Western Palearctic (Europe, North Africa, and western Asia).

Analysis of population structure

We conducted a PCA of variation among Western Palearctic individuals ($n = 357$; Fig. 2 and fig. S4). Because excessive linkage disequilibrium (LD) among genetic markers can lead to PC(s) of LD structure rather than population structure (*73*), we used Plink v.1.90 (*74*) to select a subset of 503,921 unlinked SNPs (--indep-pairwise 200 20 0.2). We then used PCAngsd v.1.10 (*75*) to estimate a covariance matrix and the princomp function in the R package stats v.3.6.2 to conduct the PCA (*76*).

Sequencing and analysis of historical specimens from London

To understand the relationship between historical and contemporary *molestus* populations, we extracted genomic DNA from 22 pinned *Culex* specimens in the National History Museum, London (table S2) using a recently published, minimally destructive protocol (*33*). Briefly, pinned specimens were removed from the main label pins and put in a styrofoam box filled with wet paper towels for rehydration at 37°C for 3 hours. Each rehydrated sample was then dipped in 200 µl of Lysis Buffer C (200 mM Tris, 25 mM EDTA, 0.05% Tween-20, and 0.4 mg/ml Proteinase K) and incubated at 37°C for 2 hours. Genomic DNA in the lysis buffer was then purified using a modified MinElute (Qiagen) silica column approach. After extraction, intact mosquito specimens were rinsed in increasing percentages of ethanol (30% and 50%) and sent back to the museum for critical point drying. Libraries of the purified genomic DNA were created using NEB Next Ultra II DNA Library Prep Kit (New England Biolabs) with no shearing and then purified using 2.2× SPRI (Beckman Coulter Agencourt AMPure XP) beads after library ligation and two times 1× SPRI after PCR amplification using a KAPA HiFi HotStart Uracil+ ReadyMix PCR Kit. The final libraries were sequenced on one lane of NovaSeq PE75 (Illumina).

Raw reads were run though the ancient DNA pipeline EAGER (*77*), with the following processing parameters: trimming adapter sequence, trimming bases of quality score <20, removing sequences shorter than 30 bp, merging overlapping paired reads (with default minimum 11-bp overlap), aligning to the CpipJ5 assembly (*62*) using BWA-MEM, removing PCR duplicates and unaligned reads for final BAM files, and performing DamageProfiler to summarize ancient DNA characteristics (50 C > T and 30 G > A substitutions, read length in base pairs). We calculated genome-wide coverage after deduplication using Mosdepth (*69*) (mean = 5.77×, range = 1.05 to 9.22×). We used ANGSD v.0.936 (*78*) to call genotype likelihoods (angsd -GL 1, SAMtools model) for the historical samples at the subset of 503,921 unlinked, biallelic SNPs used for PCA of contemporary genomes (see above). We then merged these samples with the contemporary Western Palearctic sample and conducted a joint PCA as described above (PCAngsd followed by princomp).

Analysis of latitudinal gradient

We modeled each *pipiens* population in the Western Palearctic as a mix of northern *pipiens* and *molestus* populations using genome-wide *f3* statistics (Fig. 3, A to C). Specifically, we used the threepop function in Treemix v1.13 (*79*) to calculate *f3*(X; *pipiens*, *molestus*), where X represents a focal *pipiens* population, and the *pipiens* and *molestus* reference populations came from Sweden (SWE) and Belgium (BVR), respectively. We used a block jackknife approach to obtain the standard error and compute *Z* scores, dividing the genome into blocks of 500 SNPs (-k 500). A *Z* score of −3 was used as a significance threshold (*79*).

We also estimated the number of derived alleles shared by focal *pipiens* populations with the same northern *pipiens* and *molestus* reference populations using Dsuite Dtrios (*80*), with *Cx. torrentium* as an outgroup. We specifically calculated the number of derived alleles shared with *molestus* as a fraction of those shared with either *pipiens* or *molestus*: $n(\text{ABBA})/[n(\text{ABBA}) + n(\text{BBAA})]$ where A represents the ancestral allele and B represents the derived allele as in the tree shown in Fig. 3D.

Distance (*Dxy*) tree inference

We inferred a distance tree for all *Cx. pipiens s. s.* mosquitoes with >10× genome wide coverage from the full global sample based on the number of pairwise nucleotide differences (*Dxy*). A *Cx. torrentium* individual was included as an outgroup. As hybridization can confound

relationships in distance trees, we used a variety of methods to identify and exclude populations or individuals that showed signs of admixture. Using *f3* tests we found that no *molestus* populations were well modeled as a mixture of *pipiens* and *molestus* (fig. S6), suggesting that introgression from *pipiens* into *molestus* is generally rare. However, a more sensitive four-population test (Patterson's *D*) found small yet significant signs of introgression into some Mediterranean *molestus* populations (fig. S7), which we then excluded from the tree. Identification of *pipiens* populations that have received genetic input from *molestus* is more challenging because introgression is confounded by the ancestral genetic gradient (Fig. 3). To overcome this, we used the *f*-branch statistics (*43*) as presented in Fig. 5A (see "Quantifying gene flow from *molestus* into *pipiens*" for details) and then excluded all *pipiens* populations that showed nonzero introgression. Finally, we excluded any *pipiens* or *molestus* individual with >2% inferred ancestry from sibling species *Cx. quinquefasciatus* based on an NGSadmix (*75*) analysis. Briefly, we ran NGSadmix on the LD-pruned biallelic SNP set (see "Analysis of population structure") to infer individual ancestry proportions for 707 unrelated *Cx. pipiens*, *Cx. pallens*, and *Cx. quinquefasciatus* individuals. Nine *Cx. pipiens* individuals from sub-Saharan Africa were excluded from the NGSadmix analysis as they are known to be reproductively isolated from *Cx. quinquefasciatus*. When analyzed with K = 3, the three clusters corresponded to *Cx. quinquefasciatus*, *pipiens* from northern latitudes, and *molestus*/*pipiens* from the Mediterranean. As expected, *Cx. quinquefasciatus* ancestry was rare in the Western Palearctic (*81*) but extremely common in the Americas and Asia, leading to exclusion of most, but not all, samples from these other geographic regions. After filtering, we moved forward with *Dxy* tree inference for $n = 204$ *Cx. pipiens s. s.* and $n = 1$ outgroup.

We used pixy v.1.2.7 (*82*) to estimate pairwise genome-wide *Dxy* among the samples. We included invariant accessible sites in addition to the full set of 30.6 million biallelic SNPs as exclusion of invariant sites is known to generate bias (*82*). We bootstrapped genome-wide *Dxy* estimates 100 times by sampling 1-Mb windows with replacement. We then built the genome-wide neighbor-joining tree as well as bootstrapped trees based on the resulting matrices of *Dxy* values using the R packages ape v.5.6.2 (*83*) and ggtree v3.6.2 (*84*).

We annotated populations in the tree based on microhabitat of origin—aboveground, belowground, or "suspected belowground." Suspected belowground populations included one Belgian population (BVR) and one Chinese population (BEJ). The Belgian individuals were collected aboveground in a heavily industrialized zone and suspected of having escaped from a nearby tire factory. The Chinese individuals were collected trying to bite the collector inside a residential building in Tangshan, near Beijing.

Genetic diversity (π)

We calculated genome-wide nucleotide diversity (π) for all *molestus* populations included in the *Dxy* tree analysis using pixy v.1.2.7 (*82*). A potential concern in doing so was that the eastern Mediterranean *molestus* populations, including key populations from Egypt and Israel, might have experienced introgression from *Cx. quinquefasciatus* below the 2% threshold that we used for exclusion from the tree (*81*). Even a small amount of introgression from the divergent *Cx. quinquefasciatus* could inflate diversity estimates. To identify putatively introgressed genomic regions, we used Dsuite Dtrios to calculate *f4* admixture ratios in nonoverlapping windows of fixed size (50 kb, 150 kb, 250 kb, 500 kb, 1 Mb) using the following tree: (((*pipiens*, X), *quinquefasciatus*), outgroup). Reference *pipiens* and *quinquefasciatus* populations came from Sweden (SWE) and Saudi Arabia (JED). *Cx. torrentium* was used as the outgroup. Almost all windows in most individuals showed 0 introgression, but we observed a minor peak at $f4 \sim 0.5$ in some samples (fig. S9), likely representing the heterozygous state for introgressed haplotypes. Homozygous *quinquefasciatus* haplotypes ($f4 \sim 1$) were also sometimes present, but extremely rare. After comparing signal-to-noise ratios, we settled on a window size of 150 kb and an *f4* cutoff of 0.2 for calling introgression (fig. S9). When computing diversity (π), we masked every 150-kb locus for which any of the 99 *molestus* individuals showed substantial introgression from *quinquefasciatus*. In total, we masked ~5% of all 30.6 million accessible sites.

Cross-coalescent analysis of *pipiens-molestus* split time

To estimate the divergence time between *pipiens* and *molestus*, we carried out cross-coalescent analyses using MSMC2 following published best practices (*39*, *85*). Because MSMC2 requires phased genomes, we assembled a genome phasing panel using 551 individuals with >10× coverage that represent all major geographic regions where *pipiens* and *molestus* occur (mean coverage = 19.6×, range = 10 to 87.3×). We considered the full set of 30.6 million biallelic SNPs but further filtered out genotypes with DP < 8. We first individually phased nearby heterozygous sites based on information present in sequencing reads using HAPCUT2 (*86*). This read-based phasing alone was able to phase up to ~90% of variants in the highest-coverage samples (range = 0.8 to 90.2%, median = 22.9%). We then carried out statistical phasing with the prephased variants across all individuals using SHAPEIT4 v2.2 (*87*) with a phase set error rate of 0.0001. To increase accuracy, we increased the MCMC iterations in SHAPEIT4 from the default value of 15 to 27 (--mcmc-iterations 10b + 1p + 1b + 1p + 1b + 1p + 1b + 1p + 10m), and we increased PBWT depth from the default value of 4 to 8. We phased variants on each chromosome separately. Although MSMC2 is known to be generally robust to phase-switch errors (*85*), these may be common across longer distances, generating uncertainty that should be considered when interpreting results.

We selected two high-coverage individuals from an Egyptian *molestus* population (ADR, 47.5× and 56× coverage) and another two from a Moroccan *pipiens* population (MAK, 56.1× and 67.5×). We first extracted phased genomes of focal individuals using BCFtools and generated chromosome-specific masks based on average coverage using bamCaller.py (*85*). We also masked every 150-kb locus at which the individuals showed signs of introgression from *quinquefasciatus* (see above, $f4 > 0.2$; fig. S9). We then ran MSMC2 to characterize rates of cross-coalescence within and between the two populations. The time at which the relative rate of cross-coalescence exceeded 50% was used as a point estimate of the split time (*39*). We bootstrapped MSMC2 analyses using 100 replicates of three 200-Mb "chromosomes," each composed of resampled blocks of 10 Mb. To explore the robustness of our results to sample selection, we reran the analysis with an alternative Mediterranean *pipiens* population for which high-coverage genomes were available (MEG, Armenia; 50.8× and 20.7×) (fig. S10).

MSMC2 generates split time estimates in coalescent units (*85*), which can be converted to years given a taxon-specific mutation rate (μ) and generation time (g). Because μ and g have not been directly measured in natural *Cx. pipiens* populations, we used plausible, literature-based, best-guess values, as well as biologically reasonable minima and maxima. For μ, we considered published data from mosquitoes and other insects and set the reasonable range at 1.0 to 8.0×10^{-9} (*88*–*90*). Our best guess of μ was 4.85×10^{-9}, taken from a recent estimate in *A. aegypti*, a well-studied mosquito from the same subfamily (*55*). For g, our best guess was 20 days, based on a study of an autogenous *molestus* laboratory colony (20 to 21.3 days) (*91*). However, laboratory conditions are often better than those found in nature (e.g., unlimited food), and *pipiens* mosquitoes might be delayed in finding blood meals. We therefore extended the reasonable range up to 30 days. Taken together, we used the following combinations of parameters for conversion of coalescent units to our best-guess, minimum, and maximum chronological split times (Fig. 4D): $\mu = 4.85 \times 10^{-9}$ and $g = 20$ (best-guess split time), $\mu = 8 \times 10^{-9}$ and $g = 20$ (minimum split time), $\mu = 1 \times 10^{-9}$ and $g = 30$ (maximum split time).

Quantifying gene flow from *molestus* into *pipiens*

To quantify gene flow from *molestus* into *pipiens* across the Western Palearctic while accounting for the ancestral genetic gradient, we used Dsuite Fbranch to calculate branch-specific *f4* admixture ratios (*43*) (Fig. 5 and fig. S11). We specified the tree shown in Fig. 5B and estimated gene flow into focal *pipiens* populations from the three other branches. Latitudinally varying gene flow from a northern *pipiens* population (SWE, Sweden, arrow 1) accounted for the ancestral gradient. Gene flow from a Middle Eastern *molestus* population (ADR, Egypt, arrow 2) and a northern *molestus* population (BVR, Belgium, arrow 3) allowed us to isolate genetic input from *molestus* subsequent to the split with *pipiens*.

We used a linear modeling framework to explore a potential association between *molestus* gene flow (Fig. 5D) and human population density (a proxy for urbanization). We first downloaded 30-s-resolution population density data from the Gridded Population of the World v4 (*92*) and compared the effect of density on introgression when averaging density within circles of the following radii (centered around collection sites): 1, 2, 3, 4, 5, 6, 7, 8, 9, 10, 11, 12, 13, 14, 15, 16, 17, 18, 19, 20, 30, 40, 50, 60, 70, 80, 90, and 100 km. In a simple linear regression excluding three outlier populations (PAR, LND, FON, Cook's distance > 4), human density had a significant effect using radii of 1 to 10 km, but not across larger distances (Fig. 5E). The model with human density averaged across a 3-km buffer explained the most variance ($R^2 = 0.21$) and was used in the analysis shown in Fig. 5F. We also asked whether climate could explain additional variance in *molestus* introgression across populations by adding WorldClim2 bioclimatic variables (Bio1 to Bio19) (*93*) to the human density only model one at a time, again in a linear modeling framework. None of the bioclimatic variables significantly improved the model. Bio8 (mean temperature of the wettest quarter) was the only variable that had a marginal effect (linear model $P = 0.09$).

Illustration credits

Illustrations used in Fig. 4C and Fig. 5A are downloaded and modified from Freepik.com (Wheat), Vecteezy.com (Pharaoh and Glacier), and Phylopic.com (bird and human).

REFERENCES AND NOTES

1. M. T. J. Johnson, J. Munshi-South, Evolution of life in urban environments. *Science* **358**, eaam8327 (2017). doi: 10.1126/science.aam8327; pmid: 29097520
2. H. Ritchie, V. Samborska, M. Roser, Urbanization (Our World in Data, 2024); https://ourworldindata.org/urbanization.
3. E. B. Vinogradova, *Culex Pipiens Pipiens Mosquitoes: Taxonomy, Distribution, Ecology, Physiology, Genetics, Applied Importance and Control* (Pensoft, 2000).
4. A. Farajollahi, D. M. Fonseca, L. D. Kramer, A. Marm Kilpatrick, "Bird biting" mosquitoes and human disease: A review of the role of *Culex pipiens* complex mosquitoes in epidemiology. *Infect. Genet. Evol.* **11**, 1577–1585 (2011). doi: 10.1016/j.meegid.2011.08.013; pmid: 21875691
5. R. E. Harbach, *Culex pipiens*: Species versus species complex – Taxonomic history and perspective. *J. Am. Mosq. Control Assoc.* **28**, 10–23 (2012). doi: 10.2987/8756-971X-28.4.10; pmid: 23401941
6. K. Byrne, R. A. Nichols, *Culex pipiens* in London Underground tunnels: Differentiation between surface and subterranean populations. *Heredity* **82**, 7–15 (1999). doi: 10.1038/sj.hdy.6884120; pmid: 10200079
7. A. P. Hendry, K. M. Gotanda, E. I. Svensson, Human influences on evolution, and the ecological and societal consequences. *Phil. Trans. R. Soc. B* **372**, 20160028 (2017). doi: 10.1098/rstb.2016.0028; pmid: 27920373
8. K. A. Thompson, L. H. Rieseberg, D. Schluter, Speciation and the City. *Trends Ecol. Evol.* **33**, 815–826 (2018). doi: 10.1016/j.tree.2018.08.007; pmid: 30297245
9. S. P. Otto, Adaptation, speciation and extinction in the Anthropocene. *Proc. R. Soc. B* **285**, 20182047 (2018). doi: 10.1098/rspb.2018.2047; pmid: 30429309
10. L. R. Rivkin *et al.*, A roadmap for urban evolutionary ecology. *Evol. Appl.* **12**, 384–398 (2019). doi: 10.1111/eva.12734; pmid: 30828362
11. D. N. Reznick, J. Losos, J. Travis, From low to high gear: There has been a paradigm shift in our understanding of evolution. *Ecol. Lett.* **22**, 233–244 (2019). doi: 10.1111/ele.13189; pmid: 30478871
12. P. G. Shute, Culex molestus. *Trans. R. Entomol. Soc. Lond.* **102**, 380–382 (1951). doi: 10.1111/j.1365-2311.1951.tb00758.x
13. C. Wesenberg-Lund, *Contributions to the Biology of the Danish Culicidae* (A. F. Høst and Søn, 1920).
14. J. Legendre, Le moustique cavernicole ou l'adaptation de "*Culex pipiens*" à l'urbanisme moderne. *Bull. Acad. Med.* **106**, 86–89 (1931).
15. O. Hecht, Experimentelle beiträge zur biologie der stechmücken II. *Z. Angew. Entomol.* **19**, 579–607 (1932). doi: 10.1111/j.1439-0418.1932.tb00323.x
16. D. N. Reznick, *The "Origin" Then and Now: An Interpretive Guide to the "Origin of Species"* (Princeton Univ. Press, 2012).
17. B. Nye, in *Undeniable: Evolution and the Science of Creation*, C. S. Powell, Ed. (Macmillan, 2014), pp. 137–144.
18. "Humans artificially drive evolution of new species," *EurekAlert!*, 28 June 2016; https://www.eurekalert.org/news-releases/898070.
19. E. Blakemore, "The London Underground Has Its Own Mosquito Subspecies," *Smithsonian Magazine*, 25 March 2016; https://www.smithsonianmag.com/smart-news/london-underground-has-its-own-mosquito-subspecies-180958566/.
20. K. Silver, "The unique mosquito that lives in the London Underground," *BBC*, 23 March 2016; https://www.bbc.com/earth/story/20160323-the-unique-mosquito-that-lives-in-the-london-underground [accessed 28 January 2025].
21. M. Schilthuizen, *Darwin Comes to Town: How the Urban Jungle Drives Evolution* (Picador, 2019).
22. D. M. Fonseca *et al.*, Emerging vectors in the *Culex pipiens* complex. *Science* **303**, 1535–1538 (2004). doi: 10.1126/science.1094247; pmid: 15001783
23. Y. Haba, L. McBride, Origin and status of *Culex pipiens* mosquito ecotypes. *Curr. Biol.* **32**, R237–R246 (2022). doi: 10.1016/j.cub.2022.01.062; pmid: 35290776
24. P. Forskål, *Descriptiones Animalium, Avium, Amphibiorum, Piscium, Insectorum, Vermium: Quae in Itinere Orientali Observavit* (Hauniae, 1775).
25. E. F. Germar, *Reise nach Dalmatien und in das Gebiet von Ragusa* (F. A. Brockhaus, 1817).
26. E. Ficalbi, Notizie preventive sulle zanzare Italiane. *Boll. Soc. Entomol. Ital.* **21**, 124–131 (1890).
27. K. M. Winchell, J. B. Losos, B. C. Verrelli, Urban evolutionary ecology brings exaptation back into focus. *Trends Ecol. Evol.* **38**, 719–726 (2023). doi: 10.1016/j.tree.2023.03.006; pmid: 37024381
28. F. Villani, S. Urbanelli, A. Gad, S. Nudelman, L. Bullini, Electrophoretic variation of *Culex pipiens* from Egypt and Israel. *Biol. J. Linn. Soc. Lond.* **29**, 49–62 (1986). doi: 10.1111/j.1095-8312.1986.tb01770.x
29. L. R. Petersen, A. C. Brault, R. S. Nasci, West Nile virus: Review of the literature. *JAMA* **310**, 308–315 (2013). doi: 10.1001/jama.2013.8042; pmid: 23860989
30. C. Giesen *et al.*, A systematic review of environmental factors related to WNV circulation in European and Mediterranean countries. *One Health* **16**, 100478 (2023). doi: 10.1016/j.onehlt.2022.100478; pmid: 37363246
31. M. L. Aardema, S. K. Olatunji, D. M. Fonseca, The enigmatic *Culex pipiens* (Diptera: Culicidae) species complex: Phylogenetic challenges and opportunities from a notoriously tricky mosquito group. *Ann. Entomol. Soc. Am.* **115**, 95–104 (2022). doi: 10.1093/aesa/saab038
32. See the Materials and methods.
33. P. Korlević *et al.*, A minimally morphologically destructive approach for DNA retrieval and whole-genome shotgun sequencing of pinned historic dipteran vector species. *Genome Biol. Evol.* **13**, evab226 (2021). doi: 10.1093/gbe/evab226; pmid: 34599327
34. B. Gomes *et al.*, Asymmetric introgression between sympatric *molestus* and *pipiens* forms of *Culex pipiens* (Diptera: Culicidae) in the Comporta region, Portugal. *BMC Evol. Biol.* **9**, 262 (2009). doi: 10.1186/1471-2148-9-262; pmid: 19895687
35. S. Urbanelli *et al.*, in *Atti del Primo Congresso Nazionale della Società Italiana di Ecologia*, A. Moroni, O. Ravera, A. Anelli, Eds. (Zara, 1981), pp. 305–316.
36. N. Patterson *et al.*, Ancient admixture in human history. *Genetics* **192**, 1065–1093 (2012). doi: 10.1534/genetics.112.145037; pmid: 22960212
37. S. Nudelman, R. Galun, U. Kitron, A. Spielman, Physiological characteristics of *Culex pipiens* populations in the Middle East. *Med. Vet. Entomol.* **2**, 161–169 (1988). doi: 10.1111/j.1365-2915.1988.tb00066.x; pmid: 2980171
38. O. Olsson, *Paleoeconomics: Climate Change and Economic Development in Prehistory* (Springer, 2024), pp. 285–308.
39. S. Schiffels, K. Wang, MSMC and MSMC2: The Multiple Sequentially Markovian Coalescent. *Methods Mol. Biol.* **2090**, 147–166 (2020). doi: 10.1007/978-1-0716-0199-0_7; pmid: 31975167
40. S. Huang *et al.*, Genetic variation associated with mammalian feeding in *Culex pipiens* from a West Nile virus epidemic region in Chicago, Illinois. *Vector Borne Zoonotic Dis.* **9**, 637–642 (2009). doi: 10.1089/vbz.2008.0146; pmid: 19281434
41. A. M. Kilpatrick *et al.*, Genetic influences on mosquito feeding behavior and the emergence of zoonotic pathogens. *Am. J. Trop. Med. Hyg.* **77**, 667–671 (2007). doi: 10.4269/ajtmh.2007.77.667; pmid: 17978068
42. M. L. Fritz, E. D. Walker, J. R. Miller, D. W. Severson, I. Dworkin, Divergent host preferences of above- and below-ground *Culex pipiens* mosquitoes and their hybrid offspring. *Med. Vet. Entomol.* **29**, 115–123 (2015). doi: 10.1111/mve.12096; pmid: 25600086
43. M. Malinsky *et al.*, Whole-genome sequences of Malawi cichlids reveal multiple radiations interconnected by gene flow. *Nat. Ecol. Evol.* **2**, 1940–1955 (2018). doi: 10.1038/s41559-018-0717-x; pmid: 30455444

44. M. Di Luca *et al.*, Ecological distribution and CQ11 genetic structure of *Culex pipiens* complex (Diptera: Culicidae) in Italy. *PLOS ONE* **11**, e0146476 (2016). doi: 10.1371/journal.pone.0146476; pmid: 26741494
45. H. C. Osório, L. Zé-Zé, F. Amaro, A. Nunes, M. J. Alves, Sympatric occurrence of *Culex pipiens* (Diptera, Culicidae) biotypes *pipiens, molestus* and their hybrids in Portugal, Western Europe: Feeding patterns and habitat determinants. *Med. Vet. Entomol.* **28**, 103–109 (2014). doi: 10.1111/mve.12020; pmid: 23786327
46. J. Martínez-de la Puente *et al.*, *Culex pipiens* forms and urbanization: Effects on blood feeding sources and transmission of avian *Plasmodium*. *Malar. J.* **15**, 589 (2016). doi: 10.1186/s12936-016-1643-5; pmid: 27931226
47. Eurostat, Glossary: Urban centre (2018); https://ec.europa.eu/eurostat/statistics-explained/index.php?title=Glossary:Urban_centre.
48. O. Duron *et al.*, Transposable element polymorphism of *Wolbachia* in the mosquito *Culex pipiens*: Evidence of genetic diversity, superinfection and recombination. *Mol. Ecol.* **14**, 1561–1573 (2005). doi: 10.1111/j.1365-294X.2005.02495.x; pmid: 15813794
49. E. Dumas *et al.*, Population structure of *Wolbachia* and cytoplasmic introgression in a complex of mosquito species. *BMC Evol. Biol.* **13**, 181 (2013). doi: 10.1186/1471-2148-13-181; pmid: 24006922
50. K. L. Knight, A. A. Abdel-Malek, A morphological and biological study of *Culex pipiens* in the Cairo area of Egypt (Diptera-Culicidae). *Bull. Soc. Fouad Entomol.* **35**, 175–185 (1951).
51. A. Harpak *et al.*, Genetic adaptation in New York City rats. *Genome Biol. Evol.* **13**, evaa247 (2021). doi: 10.1093/gbe/evaa247; pmid: 33211096
52. L. Weissbrod *et al.*, Origins of house mice in ecological niches created by settled hunter-gatherers in the Levant 15,000 y ago. *Proc. Natl. Acad. Sci. U.S.A.* **114**, 4099–4104 (2017). doi: 10.1073/pnas.1619137114; pmid: 28348225
53. A. Wada-Katsumata, J. Silverman, C. Schal, Changes in taste neurons support the emergence of an adaptive behavior in cockroaches. *Science* **340**, 972–975 (2013). doi: 10.1126/science.1234854; pmid: 23704571
54. M. Ravinet *et al.*, Signatures of human-commensalism in the house sparrow genome. *Proc. R. Soc. B* **285**, 20181246 (2018). doi: 10.1098/rspb.2018.1246; pmid: 30089626
55. N. H. Rose *et al.*, Dating the origin and spread of specialization on human hosts in *Aedes aegypti* mosquitoes. *eLife* **12**, e83524 (2023). doi: 10.7554/eLife.83524; pmid: 36897062
56. J. A. Rioux, J. M. Pech, Le biotype autogène de *Culex pipiens* L. ne doit pas être nommé *Culex molestus* Forskal (Diptera Culicidae). *Cahiers Des Nat.* **15**, 115–117 (1959).
57. C. M. Bahnck, D. M. Fonseca, Rapid assay to identify the two genetic forms of *Culex* (*Culex*) *pipiens* L. (Diptera: Culicidae) and hybrid populations. *Am. J. Trop. Med. Hyg.* **75**, 251–255 (2006). doi: 10.4269/ajtmh.2006.75.2.0750251; pmid: 16896127
58. E. Roubaud, Le pouvoir autogène chez le biotype nord-africain du moustique commun *Culex pipiens* (L.). *Bull. Soc. Pathol. Exot.* **36**, 172–175 (1939).
59. M. Naddaf, Mosquito-borne diseases are surging in Europe – How worried are scientists? *Nature* **633**, 749 (2024). doi: 10.1038/d41586-024-03031-y; pmid: 39284997
60. US Centers for Disease Control and Prevention (CDC), "West Nile Virus: Current Year Data (2024)" (2024); https://www.cdc.gov/west-nile-virus/data-maps/current-year-data.html.
61. A. A. Yurchenko *et al.*, Genomic differentiation and intercontinental population structure of mosquito vectors *Culex pipiens pipiens* and *Culex pipiens molestus*. *Sci. Rep.* **10**, 7504 (2020). doi: 10.1038/s41598-020-63305-z; pmid: 32371903
62. S. S. Ryazansky *et al.*, The chromosome-scale genome assembly for the West Nile vector *Culex quinquefasciatus* uncovers patterns of genome evolution in mosquitoes. *BMC Biol.* **22**, 16 (2024). doi: 10.1186/s12915-024-01825-0; pmid: 38273363
63. J. L. Smith, D. M. Fonseca, Rapid assays for identification of members of the *Culex* (*Culex*) *pipiens* complex, their hybrids, and other sibling species (Diptera: Culicidae). *Am. J. Trop. Med. Hyg.* **70**, 339–345 (2004). doi: 10.4269/ajtmh.2004.70.339; pmid: 15100444
64. S. Andrews, FastQC: A quality control tool for high throughput sequence data (2010); http://www.bioinformatics.babraham.ac.uk/projects/fastqc/.
65. A. M. Bolger, M. Lohse, B. Usadel, Trimmomatic: A flexible trimmer for Illumina sequence data. *Bioinformatics* **30**, 2114–2120 (2014). doi: 10.1093/bioinformatics/btu170; pmid: 24695404
66. H. Li, R. Durbin, Fast and accurate short read alignment with Burrows-Wheeler transform. *Bioinformatics* **25**, 1754–1760 (2009). doi: 10.1093/bioinformatics/btp324; pmid: 19451168
67. Broad Institute, Picard, v.2.20.2 (2019); http://broadinstitute.github.io/picard/.
68. G. van der Auwera, B. D. O'Connor, *Genomics in the Cloud: Using Docker, GATK, and WDL in Terra* (O'Reilly Media, 2020).
69. B. S. Pedersen, A. R. Quinlan, Mosdepth: Quick coverage calculation for genomes and exomes. *Bioinformatics* **34**, 867–868 (2018). doi: 10.1093/bioinformatics/btx699; pmid: 29096012
70. P. Danecek *et al.*, Twelve years of SAMtools and BCFtools. *Gigascience* **10**, giab008 (2021). doi: 10.1093/gigascience/giab008; pmid: 33590861
71. GATK Team, Hard-filtering germline short variants (2024); https://gatk.broadinstitute.org/hc/en-us/articles/360035890471-Hard-filtering-germline-short-variants.
72. K. Hanghøj, I. Moltke, P. A. Andersen, A. Manica, T. S. Korneliussen, Fast and accurate relatedness estimation from high-throughput sequencing data in the presence of inbreeding. *Gigascience* **8**, giz034 (2019). doi: 10.1093/gigascience/giz034; pmid: 31042285
73. A. Abdellaoui *et al.*, Population structure, migration, and diversifying selection in the Netherlands. *Eur. J. Hum. Genet.* **21**, 1277–1285 (2013). doi: 10.1038/ejhg.2013.48; pmid: 23531865
74. S. Purcell *et al.*, PLINK: A tool set for whole-genome association and population-based linkage analyses. *Am. J. Hum. Genet.* **81**, 559–575 (2007). doi: 10.1086/519795; pmid: 17701901
75. L. Skotte, T. S. Korneliussen, A. Albrechtsen, Estimating individual admixture proportions from next generation sequencing data. *Genetics* **195**, 693–702 (2013). doi: 10.1534/genetics.113.154138; pmid: 24026093
76. R Core Team, R: A Language and Environment for Statistical Computing (R Foundation for Statistical Computing, 2020); https://www.R-project.org/.
77. J. A. Fellows Yates *et al.*, Reproducible, portable, and efficient ancient genome reconstruction with nf-core/eager. *PeerJ* **9**, e10947 (2021). doi: 10.7717/peerj.10947; pmid: 33777521
78. T. S. Korneliussen, A. Albrechtsen, R. Nielsen, ANGSD: Analysis of next generation sequencing data. *BMC Bioinformatics* **15**, 356 (2014). doi: 10.1186/s12859-014-0356-4; pmid: 25420514
79. J. K. Pickrell, J. K. Pritchard, Inference of population splits and mixtures from genome-wide allele frequency data. *PLOS Genet.* **8**, e1002967 (2012). doi: 10.1371/journal.pgen.1002967; pmid: 23166502
80. M. Malinsky, M. Matschiner, H. Svardal, Dsuite - Fast *D*-statistics and related admixture evidence from VCF files. *Mol. Ecol. Resour.* **21**, 584–595 (2021). doi: 10.1111/1755-0998.13265; pmid: 33012121
81. E. V. Shaikevich, E. B. Vinogradova, A. Bouattour, A. P. Gouveia de Almeida, Genetic diversity of *Culex pipiens* mosquitoes in distinct populations from Europe: Contribution of *Cx. quinquefasciatus* in Mediterranean populations. *Parasit. Vectors* **9**, 47 (2016). doi: 10.1186/s13071-016-1333-8; pmid: 26818097
82. K. L. Korunes, K. Samuk, pixy: Unbiased estimation of nucleotide diversity and divergence in the presence of missing data. *Mol. Ecol. Resour.* **21**, 1359–1368 (2021). doi: 10.1111/1755-0998.13326; pmid: 33453139
83. E. Paradis, K. Schliep, ape 5.0: An environment for modern phylogenetics and evolutionary analyses in R. *Bioinformatics* **35**, 526–528 (2019). doi: 10.1093/bioinformatics/bty633; pmid: 30016406
84. G. Yu, D. K. Smith, H. Zhu, Y. Guan, T. T.-Y. Lam, GGTREE: An R package for visualization and annotation of phylogenetic trees with their covariates and other associated data. *Methods Ecol. Evol.* **8**, 28–36 (2017). doi: 10.1111/2041-210X.12628
85. K. Wang, I. Mathieson, J. O'Connell, S. Schiffels, Tracking human population structure through time from whole genome sequences. *PLOS Genet.* **16**, e1008552 (2020). doi: 10.1371/journal.pgen.1008552; pmid: 32150539
86. P. Edge, V. Bafna, V. Bansal, HapCUT2: Robust and accurate haplotype assembly for diverse sequencing technologies. *Genome Res.* **27**, 801–812 (2017). doi: 10.1101/gr.213462.116; pmid: 27940952
87. O. Delaneau, J.-F. Zagury, M. R. Robinson, J. L. Marchini, E. T. Dermitzakis, Accurate, scalable and integrative haplotype estimation. *Nat. Commun.* **10**, 5436 (2019). doi: 10.1038/s41467-019-13225-y; pmid: 31780650
88. P. D. Keightley, R. W. Ness, D. L. Halligan, P. R. Haddrill, Estimation of the spontaneous mutation rate per nucleotide site in a *Drosophila melanogaster* full-sib family. *Genetics* **196**, 313–320 (2014). doi: 10.1534/genetics.113.158758; pmid: 24214343
89. P. D. Keightley *et al.*, Estimation of the spontaneous mutation rate in *Heliconius melpomene*. *Mol. Biol. Evol.* **32**, 239–243 (2015). doi: 10.1093/molbev/msu302; pmid: 25371432
90. I. Rashid *et al.*, Spontaneous mutation rate estimates for the principal malaria vectors *Anopheles coluzzii* and *Anopheles stephensi*. *Sci. Rep.* **12**, 226 (2022). doi: 10.1038/s41598-021-03943-z; pmid: 34996998
91. Q. Gao *et al.*, Autogeny, Fecundity, and Other Life History Traits of *Culex pipiens molestus* (Diptera: Culicidae) in Shanghai, China. *J. Med. Entomol.* **56**, 656–664 (2019). doi: 10.1093/jme/tjy228; pmid: 30605531
92. Center for International Earth Science Information Network-CIESIN-Columbia University, Gridded Population of the World, Version 4 (GPWv4): Population Density, *NASA Socioeconomic Data and Applications Center (SEDAC)* (2016). doi: 10.7927/H49C6VHW
93. S. E. Fick, R. J. Hijmans, WorldClim 2: New 1-km spatial resolution climate surfaces for global land areas. *Int. J. Climatol.* **37**, 4302–4315 (2017). doi: 10.1002/joc.5086
94. Y. Haba, YukiHaba/PipPop_molestus_origin: v.1.0.1, Zenodo (2025). doi: 10.5281/zenodo.15866183

ACKNOWLEDGMENTS

We thank members of the McBride laboratory and M. Turelli for discussion. **Funding:** This work was supported by grants or fellowships from the Masason Foundation (Y.H.), the Honjo International Scholarship Foundation (Y.H.), the Pacific Southwest Center of Excellence in Vector-borne Diseases (C.S.M.), the Society for the Study of Evolution (Rosemary Grant Advance Award to Y.H.), the Princeton High Meadows Environmental Institute (Walbridge Fund Graduate Award to Y.H.), the American Philosophical Society (Lewis and Clark Field Scholar Award to Y.H.), the Princeton Institute for International and Regional Studies (PIIRS Dissertation Fellowship to Y.H.), the New York Hideyo Noguchi Memorial Society (NY Hideyo Noguchi Memorial Scholarship to Y.H.), the Leon Levy Foundation and the New York Academy of Sciences (Leon Levy Scholarship in Neuroscience to Y.H.), and the New York Stem Cell Foundation (Robertson Investigator Award to C.S.M.). M.K.N.L. and P.K. were supported by

core funding from Wellcome (220540/Z/20/A), which also supported the historic mosquito sequencing costs. L.L. was funded by the French government's Investissement d'Avenir program, Laboratoire d'Excellence Integrative Biology of Emerging Infectious Diseases (ANR-10-LABX-62-IBEID). A.d.T. and B.C. were supported by Ministero della Ricerca (Italy), Piano Nazionale di Ripresa e Resilienza, and the European Union's Extended Partnership initiative on Emerging Infectious Diseases (project no. PE00000007). E.F. was supported by grants from Consejería de Economía, Comercio e Innovación of the Extremadura regional governments, Spain (IB10044 and IB16135). C.M. was supported by grants by Fundação para a Ciência e a Tecnologia (starting grant IF/01302/2015; GHTM UID/Multi/04413/2020; LA-REAL LA/P/0117/2020). J.B.B. was supported by the US National Institute of Allergy and Infectious Diseases (R01AI148551). Sampling and species identification in Belgium were supported by the Flemish, Walloon, and Brussels regional governments and the Federal Public Service in the context of NEHAP (MEMO project, CES-2016-02) as well as the Belgian Science Policy Office and the Department of Economy, Science and Innovation of the Flemish government. M.O.A., A.P.G.A., C.M., and M.T.N. were funded by Global Health and Tropical Medicine, a unit of the Instituto de Higiene e Medicina Tropical of the Universidade NOVA de Lisboa (GHTM UID/Multi/04413/2020; LA-REAL LA/P/0117/2020). The Russian collections were supported by the Institute of Cytology and Genetics in Novosibirsk, Russia (FWNR-2022-0015). **Author contributions:** Y.H. conceived the study, performed and analyzed experiments, and wrote the manuscript. P.K., E.M., and M.K.N.L. helped conceive, collect, and analyze data associated with archival samples from London. M.S. helped advise Y.H. and analyze experiments. N.H.R. helped conceive the study and analyze experiments. C.S.M. conceived and supervised the study, helped analyze experiments, and wrote the manuscript. All other authors collected and identified mosquitoes. All authors provided feedback on the manuscript. **Competing interests:** The authors declare no competing interests. **Data and materials availability:** All genome resequencing data associated with this study are available in the National Center for Biotechnology Information Sequence Read Archive (790 contemporary genomes, PRJNA1209100; 22 genomes from archival museum specimens, ERS10924505 to ERS10924526). Associated scripts and data are available on GitHub (https://github.com/YukiHaba/PipPop_molestus_origin) and archived on Zenodo (*94*).

PIPPOP CONSORTIUM

Matthew L. Aardema[6], Maria O. Afonso[7], Natasha M. Agramonte[8], John Albright[9], Ana Margarida Alho[10], Antonio P. G. Almeida[7], Haoues Alout[11], Bulent Alten[12], Mine Altinli[13,14], Raouf Amara Korba[15], Stefanos S. Andreadis[16], Vincent Anghel[17], Soukaina Arich[13,18], Arielle Arsenault-Benoit[19], Célestine Atyame[20], Fabien Aubry[21], Frank W. Avila[22], Diego Ayala[23,24], Rasha S. Azrag[25], Lilit Babayan[26], Allon Bear[27], Norbert Becker[28,29], Anna G. Bega[30,31], Sophia Bejarano[32], Ira Ben-Avi[33], Joshua B. Benoit[34], Saïd C. Boubidi[35], William E. Bradshaw[36], Daniel Bravo-Barriga[37,38], Rubén Bueno-Marí[39], Nataša Bušić[40], Viktoria Čabanová[41], Brittany Cabeje[32], Beniamino Caputo[42], Maria V. Cardo[43], Simon Carpenter[44], Elena Carreton[45], Mouhamadou S. Chouaïbou[46], Michelle Christian[32], Maureen Coetzee[47,48], William R. Conner[49], Anton Cornel[50], C. Lorna Culverwell[51,52], Aleksandra I. Cupina[53], Katrien De Wolf[54], Isra Deblauwe[54], Brittany Deegan[55], Sarah Delacour-Estrella[56], Alessandra della Torre[42], Debora Diaz[33], Serena E. Dool[57], Vitor L. dos Anjos[58], Sisay Dugassa[59], Babak Ebrahimi[60], Samar Y. M. Eisa[25], Nohal Elissa[61], Sahar A. B. Fallatah[62], Ary Faraji[63], Marina V. Fedorova[64], Emily Ferrill[32], Dina M. Fonseca[65], Kimberly A. Foss[66], Cipriano Foxi[67], Caio M. França[68], Stephen R. Fricker[69,70], Megan L. Fritz[19], Eva Frontera[37], Hans-Peter Fuehrer[71], Kyoko Futami[72], Enas H. S. Ghallab[73], Romain Girod[74], Mikhail I. Gordeev[75], David Greer[17], Martin Gschwind[76,77], Milehna M. Guarido[78,79], Teoh Guat Ney[80], Filiz Gunay[12], Eran Haklay[81], Alwia A. E. Hamad[25], Jun Hang[82], Christopher M. Hardy[83], Jacob W. Hartle[84], Jenny C. Hesson[85,86], Yukiko Higa[87], Christina M. Holzapfel[36], Ann-Christin Honnen[76,77], Angela M. Ionica[88], Laura Jones[44], Përparim Kadriaj[89], Hany A. Kamal[90], Colince Kamdem[91], Dmitry A. Karagodin[92], Shinji Kasai[87], Mihaela Kavran[53], Emad I. M. Khater[73], Frederik Kiene[93], Heung-Chul Kim[94], Ilias Kioulos[95], Annette Klein[93], Marko Klemenčič[96], Ana Klobučar[97], Erin Knutson[98], Constantianus J. M. Koenraadt[99], Linda Kothera[100], Pauline Kreienbühl[21], Pierrick Labbé[13,101], Itay Lachmi[102], Louis Lambrechts[21], Nediljko Landeka[103], Christopher H. Lee[104], Bryan D. Lessard[105], Ignacio Leycegui[17], Jan O. Lundström[85,86], Yoav Lustigman[102], Caitlin MacIntyre[106], Andrew J. Mackay[107], Krisztian Magori[108], Carla Maia[7], Colin A. Malcolm[109], Ralph-Joncyn O. Marquez[33], Dino Martins[110], Reem A. Masri[111], Gillian McDivitt[32], Rebekah J. McMinn[112], Johana Medina[113], Karen S. Mellor[114], Jason Mendoza[32], Enrih Merdić[40], Stacey Mesler[32], Camille Mestre[13], Homer Miranda[32], Martina Miterpáková[115], Fabrizio Montarsi[116], Anton V. Moskaev[30], Tong Mu[58], Tim W. R. Möhlmann[99], Alice Namias[13], Ivy Ng'iru[110], Marc F. Ngangué[24], Maria T. Novo[7], Laor Orshan[33], José A. Oteo[117], Yasushi Otsuka[118], Rossella Panarese[119], Claudia Paredes-Esquivel[120], Lusine Paronyan[26], Steven T. Peper[121], Dušan V. Petrić[53], Kervin Pilapil[32], Cristina Pou-Barreto[122], Sebastien J. Puechmaille[13,101,123], Ute Radespiel[124], Nil Rahola[23], Vivek K. Raman[17], Hamadouche Redouane[125], Michael H. Reiskind[126], Nadja M. Reissen[63], Benjamin L. Rice[58,127], Vincent Robert[23], Ignacio Ruiz-Arrondo[117], Ryan Salamat[32], Amy Salamone[98], M'hammed Sarih[18], Giuseppe Satta[67], Kyoko Sawabe[87], Francis Schaffner[128,129], Karen E. Schultz[130], Elena V. Shaikevich[31], Igor V. Sharakhov[111,131], Maria V. Sharakhova[111,132], Nader Shatara[133], Anuarbek K. Sibataev[134,135], Mathieu Sicard[13], Evan Smith[34], Ryan C. Smith[104], Nathalie Smitz[136], Nicolas Soriano[32], Christos G. Spanoudis[137], Christopher M. Stone[107], Liora Studentsky[34], Tatiana Sulesco[14], Luciano M. Tantely[138], La K. Thao[139], Noor Tietze[60], Ryan E. Tokarz[140], Kun-Hsien Tsai[141], Yoshio Tsuda[87], Nataša Turić[40], Melissa R. Uhran[34], Isik Unlu[113], Wim Van Bortel[54,142], Haykuhi Vardanyan[26], Laura Vavassori[76,77], Enkelejda Velo[89], Marietjie Venter[78,143], Goran Vignjević[40], Chantal B. F. Vogels[99,144], Tatsiana Volkava[145], John Vontas[95,146], Heather M. Ward[121], Nazni Wasi Ahmad[80], Mylène Weill[13], Jennifer D. West[84], Sarah S. Wheeler[147], Gregory S. White[63], Nadja C. Wipf[76,77,148], Tai-Ping Wu[149], Kai-Di Yu[150], Elke Zimmermann[124], Carina Zittra[151]

[6]Department of Biology, Montclair State University, Montclair, NJ, USA. [7]Global Health and Tropical Medicine, GHTM, LA-REAL, Instituto de Higiene e Medicina Tropical, Universidade NOVA de Lisboa, Lisboa, Portugal. [8]DeKalb County Board of Health, Decatur, GA, USA. [9]Shasta Mosquito and Vector Control District, Anderson, CA, USA. [10]Public Health Unit USP Francisco George, Primary Medical Healthcare Cluster Lisbon North, Largo Professor Arnaldo Sampaio, Lisboa, Portugal. [11]ASTRE, UMR 117, INRAE-CIRAD, Montpellier, France. [12]Hacettepe University, Faculty of Science, Department of Biology, VERG Laboratories, Beytepe, Ankara, Turkey. [13]Institut des Sciences de l'Évolution de Montpellier (UMR 5554, CNRS-UM-IRD-EPHE), Université de Montpellier, Montpellier, France. [14]Bernhard-Nocht-Institute for Tropical Medicine, Bernhard Nocht Str. 74, Hamburg, Germany. [15]Laboratory of Health and Environment, Faculty of Life and Natural Sciences and of Earth and Universe Sciences, Mohamed El Bachir El Ibrahimi University, Bordj Bou Arreridj, Algeria. [16]Institute of Plant Breeding and Genetic Resources, Hellenic Agricultural Organization - DIMITRA, Thermi, Greece. [17]Southern Nevada Health District, Las Vegas, NV, USA. [18]Service de Parasitologie et des Maladies Vectorielles, Institut Pasteur du Maroc, Casablanca, Morocco. [19]Department of Entomology, University of Maryland, College Park, MD, USA. [20]University of Reunion Island, UMR PIMIT (Processus Infectieux en Milieu Insulaire Tropical) CNRS 9192, INSERM 1187, IRD 249, University of Reunion Island, Reunion Island, France. [21]Institut Pasteur, Université Paris Cité, CNRS UMR2000, Insect-Virus Interactions Unit, Paris, France. [22]Max Planck Tandem Group in Mosquito Reproductive Biology, Universidad de Antioquia, Medellín, Colombia. [23]MIVEGEC, University of Montpellier, CNRS, IRD, Montpellier, France. [24]CIRMF, Franceville, Gabon. [25]Department of Zoology, Faculty of Science, University of Khartoum, Khartoum, Sudan. [26]National Center of Disease Control and Prevention, Ministry of Health, Yerevan, Republic of Armenia. [27]E7 Ministry of Environmental Protection, Ramla, Israel. [28]Center for Organismal Studies, University of Heidelberg, Heidelberg, Germany. [29]German Mosquito Control Association, Speyer, Germany. [30]Laboratory of Experimental Biology and Biotechnology, Scientific and Educational Center in Chernogolovka, Federal State University of Education, Moscow, Russia. [31]Vavilov Institute of General Genetics, Russian Academy of Sciences, Moscow, Russia. [32]County of San Diego, Vector Control Program, San Diego, CA, USA. [33]Ministry of Health, Jerusalem, Israel. [34]Department of Biological Sciences, University of Cincinnati, Cincinnati, OH, USA. [35]Entomology Unit, Laboratory of Parasitology, Pasteur Institute of Algeria, Algiers, Algeria. [36]Institute of Ecology and Evolution, 5289 University of Oregon, Eugene, OR, USA. [37]Parasitología, Departamento de Sanidad Animal, Facultad de Veterinaria, Universidad de Extremadura, Cáceres, Spain. [38]Department of Animal Health Department (Parasitology and Parasitic Diseases), Faculty of Veterinary Medicine, University of Córdoba, Sanidad Animal Building, Rabanales Campus, Córdoba, Spain. [39]European Center of Excellence for Vector Control, Laboratorios Lokímica - Rentokil Initial, Valencia, Spain. [40]Department of Biology, Josip Juraj Strossmayer University of Osijek, Osijek, Croatia. [41]Department of Virus Ecology, Institute of Virology, Biomedical Research Center Slovak Academy of Sciences, Bratislava, Slovakia. [42]Department of Public Health and Infectious Diseases, Sapienza University, Rome, Italy. [43]Ecología de Enfermedades Transmitidas por Vectores, Instituto de Investigación e Ingeniería Ambiental, UNSAM, CONICET, Buenos Aires, Argentina. [44]The Pirbright Institute, Ash Road, Woking, Surrey, UK. [45]Faculty of Veterinary Medicine, Research Institute of Biomedical and Health Sciences, University of Las Palmas de Gran Canaria, Las Palmas de Gran Canaria, Spain. [46]Centre Suisse de Recherches Scientifiques en Côte d'Ivoire, Abidjan, Côte d'Ivoire. [47]Wits Research Institute for Malaria, School of Pathology, Faculty of Health Sciences, University of the Witwatersrand, Johannesburg, South Africa. [48]Centre for Emerging Zoonotic and Parasitic Diseases, National Institute for Communicable Diseases, Johannesburg, South Africa. [49]Department of Evolution and Ecology, University of California, Davis, CA, USA. [50]Kearney Agricultural Research and Extension Center, Parlier, CA, USA. [51]University of Helsinki, Medicum, Department of Virology, Helsinki, Finland. [52]Department of Life Sciences, The Natural History Museum, London, UK. [53]Faculty of Agriculture, Centre of Excellence One Health Vectors and Climate, Laboratory for Medical and Veterinary Entomology, University of Novi Sad, Novi Sad, Serbia. [54]Entomology Unit, Department of Biomedical Sciences, Institute of Tropical Medicine, Antwerp, Belgium. [55]Consolidated Mosquito Abatement District, Parlier, CA, USA. [56]Department of Animal Pathology, Faculty of Veterinary Medicine at the University of Zaragoza, Zaragoza, Spain. [57]Zoological Institute and Museum, University of Greifswald, Greifswald, Germany. [58]Department of Ecology and Evolutionary Biology, Princeton University, Princeton, NJ, USA. [59]Aklilu Lemma Institute of Pathobiology, Addis Ababa University, Addis Ababa, Ethiopia. [60]Santa Clara County Vector Control District, San Jose, CA, USA. [61]Département Faune et Actions de Salubrité, Service Parisien de Santé Environnementale, Direction de la Santé Publique, Ville de Paris, Paris, France. [62]Biology Department, College of Science, Imam Abdulrahman bin Faisal University, Dammam, Kingdom of Saudi Arabia. [63]Salt Lake City Mosquito Abatement District, Salt Lake City, UT, USA. [64]Central Research Institute for Epidemiology, Moscow, Russia. [65]Center for Vector Biology, Rutgers University, New Brunswick, NJ, USA. [66]Northeast Massachusetts Mosquito Control District, Georgetown, MA, USA. [67]Istituto Zooprofilattico Sperimentale della Sardegna, Sassari, Italy. [68]Department of Biology, Southern Nazarene University, Bethany, OK, USA. [69]STEM, University of South Australia, Adelaide, South Australia, Australia. [70]Medical Entomology, Centre for Disease Control and Environmental Health, NT Health, NT, Australia. [71]Institute of Parasitology, Department of Pathobiology, University of Veterinary Medicine, Vienna, Austria. [72]Department of Vector Ecology and Environment, Institute of Tropical Medicine, Nagasaki University, Nagasaki, Japan. [73]Department of Entomology, Faculty of Science, Ain Shams University, Abbassia, Cairo, Egypt. [74]Medical Entomology Unit, Institut Pasteur de Madagascar, Antananarivo, Madagascar. [75]Department of General Biology and Ecology, Federal State University of Education, Moscow, Russia. [76]Swiss Tropical and Public Health Institute, Allschwil, Switzerland. [77]University of Basel, Basel, Switzerland. [78]Centre for Emerging and Reemerging Arbo and Respiratory Virus Research (CEARV), Department Medical Virology, University of Pretoria, South Africa. [79]Department of Production Animal Studies, Faculty of Veterinary Science, University of Pretoria, Onderstepoort, South Africa. [80]Medical Entomology Unit, Infectious Disease Research Centre, Institute For Medical Research, National Institutes of Health, Kuala Lumpur, Malaysia. [81]Ministry of Environmental Protection, Jerusalem, Israel. [82]Walter Reed Army Institute of Research, Silver Spring, MD, USA. [83]Environment, CSIRO, Canberra, Australia. [84]Placer Mosquito and Vector Control District, Roseville, CA, USA. [85]Department of Medical Biochemistry and Microbiology/Zoonosis Science Center, Uppsala University, Uppsala, Sweden. [86]Biologisk Myggkontroll, Nedre Dalälven Utvecklings AB, Uppsala, Sweden. [87]Department of Medical Entomology, National Institute of Infectious Diseases, Tokyo, Japan. [88]Department of Parasitology and Parasitic Diseases, University of Agricultural Sciences and Veterinary Medicine of Cluj-Napoca, Cluj-Napoca, Romania. [89]Vector Control Unit, Department of Epidemiology and Control of Infectious Diseases, Institute of Public Health, Tirana, Albania. [90]Department of Pest Control Projects, Dallah Company, Jeddah, Kingdom of Saudi Arabia. [91]Department of Biological Sciences, The University of Texas at El Paso, El Paso, TX, USA. [92]Institute of Cytology and Genetics, Novosibirsk, Russia. [93]Institute of Zoology and Institute of Parasitology, Centre for Infection Medicine, University of Veterinary Medicine Hannover, Hanover, Germany. [94]Force Health Protection and Preventive Medicine, Medical Department Activity-Korea/65th Medical Brigade, Unit 15281, APO AP 96271-5281, USA. [95]Department of Crop Science, Agricultural University of Athens, Athens, Greece. [96]Croatian Institute for Public Health of Međimurje County, Čakovec, Croatia. [97]Department of Epidemiology, Andrija Stampar Teaching Institute of Public Health, Zagreb, Croatia. [98]Washington State Department of Health, Olympia, WA, USA. [99]Laboratory of Entomology, Wageningen University and Research, Wageningen, Netherlands. [100]Centers for Disease Control and Prevention, Fort Collins, CO, USA. [101]Institut Universitaire de France, Paris, France. [102]Nature and Parks Authority, Jerusalem, Israel. [103]Institute of Public Health of the Istrian County, Pula, Croatia. [104]Department of Plant Pathology, Entomology and Microbiology Iowa State University, Ames, IA, USA. [105]Australian National Insect Collection, National Research Collections Australia, CSIRO, Canberra,

Australia. [106]Zoonotic Arbo- and Respiratory Virus Program, Centre for Viral Zoonoses, Faculty of Health Sciences, University of Pretoria, Pretoria, South Africa. [107]Illinois Natural History Survey, Prairie Research Institute, University of Illinois at Urbana-Champaign, Champaign, IL, USA. [108]Department of Biology, Eastern Washington University, Cheney, WA, USA. [109]School of Health, Medicine and Life Sciences, University of Hertfordshire, Hatfield, Hertfordshire, UK. [110]Mpala Research Centre, Nanyuki, Kenya. [111]Department of Entomology and Fralin Life Sciences Institute, Virginia Polytechnic and State University, Blacksburg, VA, USA. [112]Department of Microbiology, Immunology, and Pathology, Colorado State University, Fort Collins, CO, USA. [113]Miami-Dade County Mosquito Control, Miami, FL, USA. [114]Antelope Valley Mosquito and Vector Control District, Lancaster, CA, USA. [115]Institute of Parasitology, Slovak Academy of Sciences, Košice, Slovakia. [116]Laboratorio di Entomologia Sanitaria e Patogeni Trasmessi da Vettori, Istituto Zooprofilattico Sperimentale delle Venezie, Legnaro, Italy. [117]Department of Infectious Diseases, Center of Rickettsiosis and Arthropod-Borne Diseases (CRETAV), San Pedro University Hospital-Center for Biomedical Research from La Rioja (CIBIR), Logroño, Spain. [118]Research Center for the Pacific Islands, Kagoshima University, Kagoshima, Japan. [119]Dipartimento di Medicina Veterinaria, Università degli Studi di Bari, Valenzano, Italy. [120]Parasitology and Mediterranean Ecoepidemiology Research Group, University of the Balearic Islands, Palma, Spain. [121]Anastasia Mosquito Control District of St. Johns County, Augustine, FL, USA. [122]Instituto Universitario de Enfermedades Tropicales y Salud Pública de Canarias. Universidad de La Laguna, Tenerife, Spain. [123]Applied Zoology and Nature Conservation, University of Greifswald, Greifswald, Germany. [124]Institute of Zoology, University of Veterinary Medicine Hannover, Hanover, Germany. [125]Regional Health Observatories, Oran, Algeria. [126]Department of Entomology and Plant Pathology, North Carolina State University, Raleigh, NC, USA. [127]Madagascar Health and Environmental Research (MAHERY), Maroantsetra, Madagascar. [128]Francis Schaffner Consultancy, Riehen, Switzerland. [129]National Centre for Vector Entomology, Institute of Parasitology, Vetsuisse Faculty, University of Zürich, Zürich, Switzerland. [130]Mosquito and Vector Management District of Santa Barbara County, Summerland, CA, USA. [131]Department of Genetics and Cell Biology, Tomsk State University, Tomsk, Russia. [132]Laboratory of Cell Differentiation Mechanisms, Institute of Cytology and Genetics, Novosibirsk, Russia. [133]San Francisco Department of Public Health, San Francisco, CA, USA. [134]Department of Biology, Plant Protection and Quarantine, S.Seifullin Kazakh Agrotechnical Research University, Astana, Kazakhstan. [135]Department of General Biology and Genomics, Eurasian National University, Astana, Kazakhstan. [136]Royal Museum for Central Africa, Tervuren, Belgium. [137]Faculty of Agriculture, Forestry and Natural Environment, School of Agriculture, Laboratory of Applied Zoology and Parasitology, Aristotle University of Thessaloniki, Thessaloniki, Greece. [138]Unité d'Entomologie Médicale, Institut Pasteur de Madagascar, Antananarivo, Madagascar. [139]Kern Mosquito and Vector Control District, Bakersfield, CA, USA. [140]Department of International and Global Studies, Mercer University, Macon, GA, USA. [141]Department of Public Health, Institute of Environmental and Occupational Health Sciences, College of Public Health, National Taiwan University, Taipei, Taiwan. [142]Outbreak Research Team, Department of Biomedical Sciences, Institute of Tropical Medicine, Antwerp, Belgium. [143]Emerging Viral Threats, One Health Vaccines and Surveillance (EVITOH) Division, Infectious Disease and Oncology Research Institute (IDORI), University of the Witwatersrand, Johannesburg, South Africa. [144]Department of Epidemiology of Microbial Diseases, Yale School of Public Health, New Haven, CT, USA. [145]Laboratory of Parasitology, The State Scientific and Production Amalgamation, The Scientific and Practical Center of the National Academy of Sciences of Belarus for Biological Resources, Belarus, Minsk. [146]Institute Molecular Biology Biotechnology Foundation for Research and Technology, Heraklion, Crete, Greece. [147]Sacramento-Yolo Mosquito and Vector Control District, Elk Grove, CA, USA. [148]Vector Biology Department, Liverpool School of Tropical Medicine, Liverpool, UK. [149]Wuhan Center for Disease Control and Prevention, Wuhan, China. [150]Institute of Environmental and Occupational Health Sciences, College of Public Health, National Taiwan University, Taipei, Taiwan. [151]Division Limnology, Department of Functional and Evolutionary Ecology, University of Vienna, Vienna, Austria.

SUPPLEMENTARY MATERIALS

science.org/doi/10.1126/science.ady4515
Figs. S1 to S11; Tables S1 and S2; MDAR Reproducibility Checklist
Submitted 24 April 2025; accepted 3 September 2025
10.1126/science.ady4515